

Review

Kinetic Studies on the 2-Oxoglutarate/Fe(II)-Dependent Nucleic Acid Modifying Enzymes from the AlkB and TET Families

Zhiyuan Peng¹, Jian Ma¹, Christo Z. Christov², Tatyana Karabancheva-Christova², Nicolai Lehnert³  and Deyu Li^{1,*} 

¹ Department of Biomedical and Pharmaceutical Sciences, College of Pharmacy, University of Rhode Island, Kingston, RI 02881, USA

² Department of Chemistry, Michigan Technological University, Houghton, MI 49931, USA

³ Department of Chemistry and Department of Biophysics, University of Michigan, Ann Arbor, MI 48109, USA

* Correspondence: deyuli@uri.edu

Abstract: Nucleic acid methylations are important genetic and epigenetic biomarkers. The formation and removal of these markers is related to either methylation or demethylation. In this review, we focus on the demethylation or oxidative modification that is mediated by the 2-oxoglutarate (2-OG)/Fe(II)-dependent AlkB/TET family enzymes. In the catalytic process, most enzymes oxidize 2-OG to succinate, in the meantime oxidizing methyl to hydroxymethyl, leaving formaldehyde and generating demethylated base. The AlkB enzyme from *Escherichia coli* has nine human homologs (ALKBH1-8 and FTO) and the TET family includes three members, TET1 to 3. Among them, some enzymes have been carefully studied, but for certain enzymes, few studies have been carried out. This review focuses on the kinetic properties of those 2-OG/Fe(II)-dependent enzymes and their alkyl substrates. We also provide some discussions on the future directions of this field.

Keywords: kinetics; 2-OG-dependent enzyme; AlkB; ALKBH protein; FTO; TET



Citation: Peng, Z.; Ma, J.; Christov, C.Z.; Karabancheva-Christova, T.; Lehnert, N.; Li, D. Kinetic Studies on the 2-Oxoglutarate/Fe(II)-Dependent Nucleic Acid Modifying Enzymes from the AlkB and TET Families.

DNA 2023, 3, 65–84. <https://doi.org/10.3390/dna3020005>

Academic Editor: Tina Bianco-Miotto

Received: 22 December 2022

Revised: 3 March 2023

Accepted: 13 March 2023

Published: 30 March 2023



Copyright: © 2023 by the authors. Licensee MDPI, Basel, Switzerland. This article is an open access article distributed under the terms and conditions of the Creative Commons Attribution (CC BY) license (<https://creativecommons.org/licenses/by/4.0/>).

1. Introduction

DNA and RNA are modified by exogenous and endogenous chemicals, such as methyl methanesulfonate (MMS) [1], dimethyl sulfate [2], acrolein, malondialdehyde [3], S-adenosylmethionine (SAM), and PUFA (polyunsaturated fatty acids), causing a variety of modifications [4–6]. *Escherichia coli* AlkB protein is one of the four proteins (Ada, AlkA, AlkB, and AidB) induced during the adaptive response to counteract the attack of alkylating agents [7–10]. AlkB was subsequently discovered as an Fe(II)/2-oxoglutarate (or α -ketoglutarate, 2-OG or α -KG)-dependent dioxygenase (Figure 1) [11–14]. This dioxygenase uses both oxygen atoms from O₂ during the repair; one oxygen is utilized in the hydroxylated nucleic acid product and the other is used for the oxidation of the co-substrate 2-OG to succinate [15–17]. 2-OG-dependent dioxygenase was first discovered in 1967: Hutton et al. reported an oxygenase-dependent reaction catalyzed by collagen prolyl hydroxylase (CPH) that requires 2-OG [18]. Since this discovery, scientists have identified many 2-OG-dependent enzymes in the biological processes of plants and animals [19]. The TET/JBP family also belongs to the 2-OG oxygenases. The AlkB, TET and JBP family enzymes have been studied extensively for their DNA/RNA modification activities. The overall reaction mechanism of the AlkB/TET enzymes follows the general strategy of non-heme Fe(II)/2-OG enzymes that includes 2-OG binding and substrate binding, followed by dioxygen binding and activation, hydrogen atom transfer, rebound hydroxylation and product release (Figure 2) [20].

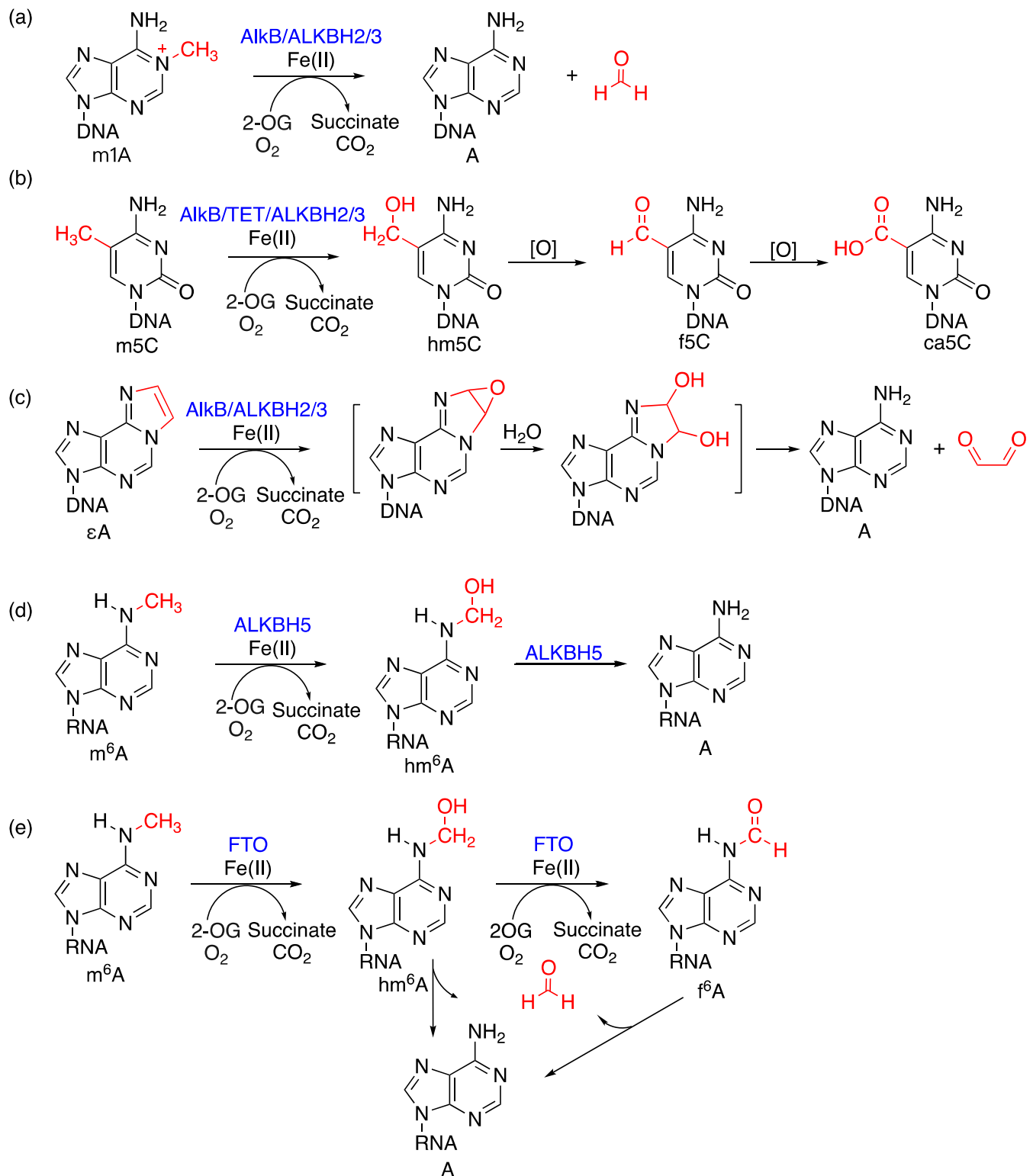


Figure 1. Proposed mechanisms of oxidative modifications on representative substrates catalyzed by 2-OG/Fe(II)-dependent dioxygenases. (a) m3C repaired by AlkB, ALKBH2 and 3; (b) m5C oxidized by AlkB, ALKBH2 and 3 and TET; (c) ϵ A repaired by AlkB; (d) m6A demethylated by ALKBH5; and (e) m6A demethylated by FTO.

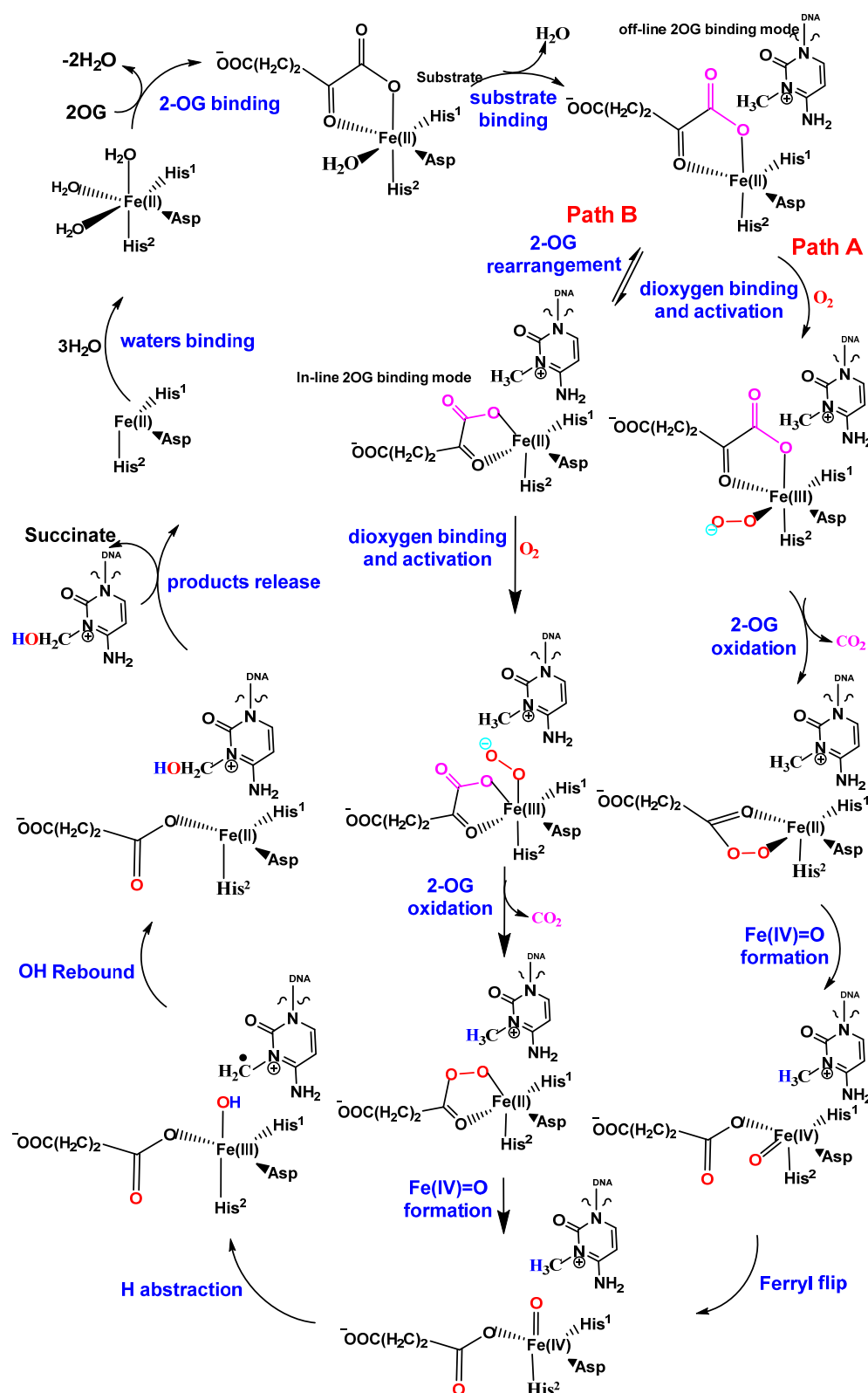


Figure 2. Proposed detailed mechanism of AlkB/TET family enzymes on monoalkyl substrates (exemplified with m3C). The steps include 2-OG binding, substrate binding, dioxygen binding and activation, 2-OG oxidation, Fe(IV)=O formation, ferryl flip, H abstraction, OH rebound, product release, water binding, etc. Adapted from Scheme 1 in [20].

Initially, AlkB was reported to oxidize 1-methyladenine (m1A) and 3-methylcytosine (m3C) in DNA, with loss of formaldehyde and recovery of the unmodified bases [13,14]. Later, this enzyme was found to repair lesions in RNA as well [11]. Other substrates include 1-methylguanine (m1G), 3-methylthymine (m3T) [21,22], N²-methylguanine (m2G) and N⁴-methylcytosine (m4C) [23], N⁶-methyladenine (m6A) [24], 1,N⁶-ethanoadenine (EA) [24], 1,N⁶-ethenoadenine (ϵ A) [25,26], and other adducts [27,28]. AlkB human homologs have been identified as ALKBH1-8 [29] and FTO [30] (also referred as ALKBH9). ALKBH2 and ALKBH3 have been reported to repair m1A and m3C in DNA [31], and ALKBH3 can also repair lesions in RNA [11]. Later, other homologs were investigated for their dealkylation activities. For example, FTO (fat mass and obesity associated [32]) was discovered to demethylate m6A in DNA or RNA (Figure 1) [33]. TET family enzymes (TET1-3) oxidize 5-methylcytosine (m5C) in DNA in successive steps to 5-hydroxymethylcytosine (hm5C), 5-formylcytosine (f5C), and 5-carboxylcytosine (ca5C) (Figure 1) [34–40]. JBP family enzymes (JBP1 and 2) can perform the oxidative hydroxylation of thymine to 5-hydroxymethyluracil (hm5U) in the biosynthesis of Base J (β -D-glucosyl-hydroxymethyluracil) [41–43]. For recent progresses on the AlkB, TET and JBP family enzymes, please see several review articles [44–47]. In order to determine whether a certain substrate is either a strong or weak substrate of a protein, kinetic study is a reliable way to distinguish them. This review mainly focuses on the kinetic behaviors of these enzymes in reactions with different DNA/RNA substrates. Some other studies aimed to investigate the enzyme–substrate complex formation and individual steps of the reaction pathways [48–50].

Non-enzymatic methylations from endogenous SAM [6] or exogenous methylating agents, such as MMS [1] and dimethyl sulfate [2], are the major sources that generate methylated modifications. Some modifications, including m3C, m1A, m1G, and m3T, are mutagenic [21], while others, including m6A, m4C and m2G in DNA, do not disrupt Watson–Crick base pairing and thus are not mutagenic [23]. Epigenetic marker m5C constitutes 60–80% of human genomic DNA on the CpG islands [51,52]; it also appears on non-CpG methylation [53]. m6A is 0.1–0.4% of total adenosine residues in cellular RNA [54]. Etheno-DNA lesions are a type of highly mutagenic and toxic biomarker; they are formed from products of either lipid peroxidation (LPO) or the carcinogen vinyl chloride and its derivatives [55]. Several etheno-DNA biomarkers, including ϵ A, 3,N⁴-ethenocytosine (ϵ C), 3,N⁴-etheno-5-methylcytosine (ϵ 5mC), 1,N²-ethenoguanine (1,N²- ϵ G), and N²,3-ethenoguanine (N²,3- ϵ G), have been characterized [56,57]. Until now, there are still many enzymes (ALKBH 4, 6, 7, 8, TET 1 and 3, and JBP1 and 2) that have not been kinetically investigated. This review aims to provide insights into the kinetic behavior of the 2-OG/Fe(II) enzymes and offers discussions on the methods of those studies. The enzymes and their substrates are summarized in Table 1, and the kinetic parameters are summarized in Tables 2–4.

Table 1. Updated DNA/RNA substrates of 2-OG/Fe(II)-dependent enzymes.

Enzyme	Substrate
AlkB	DNA: m1A, m3C, m1G, m3T, m4C, m2G, m22G, m5C, e1A, ϵ A, ϵ C, 1,N ² - ϵ G, e2G, EA, FF, HF, α HOPG, γ HOPG, M1G, HEC, HPC
	RNA: m1A, m3C, m1G,
ALKBH1	DNA: m3C, m6A
	RNA: m3C, m5C, m1A
ALKBH2	DNA: m1A, m3C, m1G, m3T, m5C, e1A, N ³ -EtdT, ϵ A, ϵ C, 1,N ² - ϵ G
ALKBH3	DNA: m1A, m3C, m3T, m5C, e1A, N ³ -EtdT, ϵ C, ϵ A
	RNA: m1A, m3C, m6A
ALKBH4	DNA: m6A
ALKBH5	RNA: m6A, m66A

Table 1. *Cont.*

Enzyme	Substrate
ALKBH6	–
ALKBH7	RNA: m1A, m22G, εA
ALKBH8	RNA: mc5mU
FTO	DNA: m3T, m6A
	RNA: m3U, m6A, m1A, m3C
TET1-3	DNA: m5C, T
	RNA: m5C

Table 2. Kinetic parameters of ALKBH1, 2, 3 and TET2 for different substrates (X: modified base).

Enzyme	DNA/ RNA	Substrate	DNA/RNA Sequence 5'-3'	K _{cat} (min ⁻¹)	K _m (μm)	K _{cat} /K _m (min ⁻¹ μm ⁻¹)	Reference
ALKBH1	DNA	m6A	ACCTTATGGAXAGCATGCTTG in ds-DNA	0.136 ± 0.0036	3.18 ± 0.28	0.04	[58]
	DNA		ACCTTATGGAXAGCATGCTTG	0.076 ± 0.0012	2.79 ± 0.18	0.03	
ALKBH2	DNA	m1A	AAAGCAGXATTCGAAAAAG CGAAA in ds-DNA	823.2 ± 120	0.320 ± 0.073	2573	[59]
	DNA		AAAGCAGXATTCGAAAAA GCGAAA	198 ± 16.2	0.183 ± 0.023	1082	
	RNA		AAAGCAGXAUUCGAA in ds-DNA	2.19 ± 0.05	0.30 ± 0.07	7.4	
	RNA	m3C	CGCGXAUUCGCG	3.67 ± 0.35	1.09 ± 0.14	3.4	[60]
	RNA		AAAGCAGXAUUCGAA	4.07 ± 0.15	0.95 ± 0.11	4.3	
	DNA		GAAGACCTXGGCGTCC in ds-DNA	2.5 ± 0.1	7.3 ± 0.9	0.34	
	DNA	m3C	GAAGACCTXGGCGTCC	1.1 ± 0.1	4.1 ± 0.9	0.27	[61]
	DNA		AAAGCACXGGTCGAAAAAGC GAAA in ds-DNA	530.4 ± 52.8	0.167 ± 0.027	3176	
	DNA		AAAGCACXGGTCGAAAAA GCGAAA	63.6 ± 7.2	0.0822 ± 0.022	774	
	DNA		GAAGACCTXGGCGTCC in ds-DNA	2.6 ± 0.1	1.9 ± 0.4	1.3	
	DNA		GAAGACCTXGGCGTCC	1.7 ± 0.1	1.4 ± 0.2	1.2	
ALKBH3	DNA	m1A	AAAGCAGXATTCGAAAAAGCG AAA in ds-DNA	109.8 ± 2.28	0.263 ± 0.110	418	[59]
	DNA		AAAGCAGXATTCGAAAAA GCGAAA	178.8 ± 44.4	0.182 ± 0.140	982	
	RNA		AAAGCAGXAUUCGAA in ds-DNA	2.57 ± 0.27	6.60 ± 0.19	0.39	
	RNA	m3C	AAAGCAGXAUUCGAA	3.56 ± 0.31	1.12 ± 0.16	3.2	[60]
	RNA		CGCGXAUUCGCG	3.13 ± 0.22	1.47 ± 0.08	2.1	
	DNA		GAAGACCTXGGCGTCC	1.2 ± 0.0	2.3 ± 0.1	0.51	
	DNA	m3C	AAAGCAGXATTCGAA	3.04 ± 0.22	0.97 ± 0.07	3.1	[61]
	DNA		AAAGCACXGGTCGAAAAAGCG AAA in ds-DNA	2.268 ± 0.462	0.0084 ± 0.016	270	
	DNA		AAAGCACXGGTCGAAAAA GCGAAA	123.6 ± 19.2	0.162 ± 0.048	763	
	DNA		GAAGACCTXGGCGTCC	1.7 ± 0.0	1.9 ± 0.4	0.87	
TET2	DNA	m5C	ACCACXGGTGGT	0.127 ± 0.019	0.48 ± 0.19	0.27	[63]
	DNA	hm5C	ACCACXGGTGGT	0.038 ± 0.005	0.90 ± 0.30	0.04	
	DNA	f5C	ACCACXGGTGGT'	0.0276 ± 0.002	1.30 ± 0.27	0.02	

Table 3. Kinetic parameters of ALKBH5 and FTO for different substrates (X: modified base).

Enzyme	DNA/ RNA	Substrate	DNA/RNA Sequence 5'-3'	K _{cat} (min ⁻¹)	K _m (μm)	K _{cat} /K _m (min ⁻¹ μm ⁻¹)	Reference
ALKBH5	RNA	m6A	AUUGUCAXCAGCAGC	0.169 ± 0.0106	1.38 ± 0.2653	0.12	[64]
	DNA		ATTGTCAXCAGCAGA	0.174 ± 0.008	1.66 ± 0.16	0.11	[65]
	RNA		UACACUCGAUCUGGXCU AAAGCU GCUC-biotin-3'	0.3 ± 0.067	2.5 ± 0.5	0.12	[66]

Table 3. Cont.

Enzyme	DNA/ RNA	Substrate	DNA/RNA Sequence 5'-3'	K_{cat} (min^{-1})	K_m (μm)	K_{cat}/K_m ($\text{min}^{-1} \mu\text{m}^{-1}$)	Reference
FTO	RNA		UACACUCGAUCUGGXCU AAAGCU GCUC-biotin-3'		0.192		
	RNA		GGXCU	0.140 ± 0.013	2.344 ± 0.140	0.06	[67]
	DNA		GAXCA	0.162 ± 0.014	2.251 ± 0.042	0.07	
	RNA		GCGGXCUCCAGAUG	0.172 ± 0.010	1.755 ± 0.088	0.1	
	RNA		CCCCXCCCCCCCCC	0.137 ± 0.021	2.583 ± 0.256	0.05	
	RNA		GGXCU-	0.16 ± 0.02	1.64 ± 0.05	0.1	[62]
	RNA		AUUGUCAXCAGCAG	0.306 ± 0.034	1.335 ± 0.213	0.23	[68]
	DNA		GGXCT	2.6 ± 0.6	1.6 ± 0.1	1.6	[69]
	RNA	m6A	AUUGUCAXCAGCAGC	0.296 ± 0.004	0.409 ± 0.023	0.72	[33]
	RNA		AUUGUCAXCAGCAGC	0.381 ± 0.114	0.6 ± 0.12	0.63	[65]
	RNA		m7GpppXCA	7.77	16.09	0.48	[70]
	RNA		m7GpppACX	0.46	6.4	0.07	
	RNA		GGXCU	0.54	9.29	0.06	
	RNA		GGXCU	0.347 ± 0.015	0.508 ± 0.126	0.68	[67]
	DNA		GGXCT	0.334 ± 0.57	0.586 ± 0.137	0.57	
	DNA		GCGGXCUCCAGAUG	0.376 ± 0.009	0.488 ± 0.074	0.77	
	RNA		CCCCXCCCCCCCCC	0.268 ± 0.012	0.688 ± 0.025	0.39	
	RNA		GGXCU	0.35 ± 0.03	0.51 ± 0.06	0.69	[62]
	RNA		AUUGUCAXCAGCAG	0.46 ± 0.055	0.59 ± 0.094	0.78	[68]
	RNA		containing 50 μM NADP	0.406 ± 0.0467	0.401 ± 0.0521	1.01	
			50 μM NADH	0.290 ± 0.0311	0.528 ± 0.0660	0.55	
			50 μM NADP+	0.282 ± 0.0340	0.961 ± 0.127	0.29	
			50 μM NAD+	0.224 ± 0.0291	1.125 ± 0.158	0.20	
			50 μM Vc	0.136 ± 0.0258	3.015 ± 0.572	0.45	
	DNA		GGXCT	0.015 ± 0.005	12 ± 2	0.01	[69]
	RNA	m6A _m	m7GpppX	8.78	1.34	6.55	[70]
	RNA	m3U	CTGACGGAGAXGAA CGTCAG		2.88		[71]
	RNA		CUUGUCAXCAGCAGA	0.115 ± 0.022	8.51 ± 3.13	0.014 ± 0.007	[72]
	DNA	m3T	CTTGTCAXCAGCAGA	0.007 ± 0.0002	0.95 ± 0.12	0.007 ± 0.002	[72]

Table 4. Kinetic parameters of *E. coli* AlkB for different substrates (X: modified base).

Enzyme	DNA/ RNA	Substrate	DNA/RNA Sequence 5'-3'	K_{cat} (min^{-1})	K_m (μm)	K_{cat}/K_m ($\text{min}^{-1} \mu\text{m}^{-1}$)	Reference
AlkB	DNA	m1A	poly(dA) methylated with [¹⁴ C]MeI	11.7 ± 0.2	1.4 ± 0.2	8.6	[73]
	DNA		TXT	7.4 ± 0.6	2.8 ± 0.9	2.6	
	DNA		TX	3.7	4.4	0.8	
	DNA		TXT	2.7 ± 0.8	1.4 ± 0.5	1.9	[74]
	DNA		CGTCGXATTCTAGAGCCCC	3.7 ± 0.2	5.4 ± 0.9	0.68	[75]
	DNA		CGTCGXATTCTAGAGCCCC in ds-DNA	3.1 ± 0.2	6.2 ± 1.3	0.48	
	DNA		TXT	2.7 ± 0.8	1.4 ± 0.9	1.9	[76]
	DNA		CAXAT	5.4 ± 1.3	0.06 ± 0.01	97	
	DNA		TXT	5.2 ± 0.2	3.2 ± 0.4	1.6	[77]
	DNA		ATTGTCAXCAGCAGA	7.41 ± 0.47	2.00 ± 0.35	3.7	[65]
	RNA		AUUGUCAXCAGCAGC	3.72 ± 0.19	2.32 ± 0.31	1.6	
	RNA		AAAGCAGXAUUCGAA in ds-DNA	2.25 ± 0.18	3.56 ± 0.24	0.63	[60]
	RNA		r(CGCGXAUUCGCG) probe	4.10 ± 0.29	1.30 ± 0.12	3.2	
	RNA		AAAGCAGXAUUCGAA	3.75 ± 0.12	1.44 ± 0.25	2.6	
	DNA		GAAGACCTXGGCGTCC	4.2 ± 0.2	7.1 ± 1.1	0.59	[61]
	DNA		GAAGACCTXGGCGTCC in ds-DNA	4.8 ± 0.2	12.7 ± 1.3	0.38	

Table 4. Cont.

Enzyme	DNA/ RNA	Substrate	DNA/RNA Sequence 5'-3'	K_{cat} (min^{-1})	K_m (μM)	K_{cat}/K_m ($\text{min}^{-1} \mu\text{M}^{-1}$)	Reference
	DNA		CGATAGCATCCTXCCTT CTCTCCAT	54 ± 1.8	0.041 ± 0.007	1317	[78]
	DNA		CGATAGCATCCTXCCTTCTC ^c in ds-DNA	46.2 ± 1.2	0.65 ± 0.05	71.1	
	DNA	m6A	ATTGTCAXCAGCAGA	0.107 ± 0.013	14.93 ± 2.46	0.01	[65]
D135S	RNA	m1G	GAGCXUUAG			2.2	[79]
D135T	RNA		GAGCXUUAG	0.052 ± 0.008	3.3 ± 1.3	15.7 ± 3.7	
	DNA	m3C	CGTCGAATTXTA GAGCCCC	2.2 ± 0.1	3.4 ± 0.6	0.65	[75]
	DNA		CGTCGAATTXTA GAGCCCC-in ds-DNA	3.3 ± 0.2	9.3 ± 2.4	0.35	
	DNA		TXT	21 ± 4	24 ± 5	0.9	[76]
	DNA		CAXAT	23 ± 10	0.29 ± 0.03	78.3	
	DNA		TTXTTTTTTTTTTTT	2.6 ± 0.3	0.0353 ± 0.0066	73.6	[80]
	DNA		CAXAT	21.2 ± 1.1	0.4 ± 0.1	53	[77]
	DNA		GAAGACCTXGGCGTCC in ds-DNA	8.2 ± 0.4	10.8 ± 1.9	0.76	[61]
	DNA		GAAGACCTXGGCGTCC	24.5 ± 0.7	19.9 ± 1.3	1.2	
	DNA		70-mer Poly T with X at position 1		2.4		[81]
	DNA		70-mer Poly T with X at position 35		6.7		
	DNA		70-mer Poly T with X at position 15		8.2		
	DNA	ϵA	TXT	0.06			[25]
	DNA		GAAGACCTXGGCGTCC	1.8			[26]
	DNA		TXT	0.13 ± 0.05	60 ± 14	0.002	[76]
	DNA		40-mer containing A treated by chloroacetaldehyde	0.134	67.4	0.0019	[82]
	DNA		CGATAGCATCCTXCCTT CTCTCCAT	45 ± 6.6	5.3 ± 1.3	8.5	[78]
	DNA		CGATAGCATCCTXCCTTCTC ^c in ds-DNA	102 ± 30	8.4 ± 3.4	12.1	

2. Kinetic Studies of the AlkB and TET Family Enzymes

2.1. ALKBH1

Initially, ALKBH1 was the first mammalian AlkB homolog identified in 1996 [83]. ALKBH1 shows strong homology with AlkB (23% identity and 59% similarity). [11,84] ALKBH1 was reported as a histone dioxygenase that modifies histone H2A methylation status [85]. ALKBH1 has also been reported to repair multiple DNA/RNA substrates: it can demethylate m3C in both DNA/ RNA [86,87] and m5C in tRNA [88,89]. Additionally, ALKBH1 is involved in the demethylation of m6A in genomic DNA [58,90] and demethylation of m1A within cytoplasmic tRNAs [91].

To the best of our knowledge, only ALKBH1-mediated oxidation of m6A and m1A have been reported with kinetic data (Table 2). It was found that ALKBH1 demethylates m6A in the single-stranded regions of the mammalian genome. First, enzymatic profiling studies have determined that ALKBH1 prefers bubbled or bulged DNAs as substrates, instead of ss-DNA or ds-DNA. Additionally, enzymatic kinetic analyses were carried out with bulged DNA ($k_{cat}/K_m = 0.043 \text{ min}^{-1} \mu\text{M}^{-1}$) compared to ss-DNA ($k_{cat}/K_m = 0.027 \text{ min}^{-1} \mu\text{M}^{-1}$) to support these findings. Kinetic studies of m1A repair by ALKBH1 were also performed [91]. In the report, since ALKBH1 has a tRNA binding motif, the authors measured the maximal velocity values of m1A demethylation toward the stem-loop probes to mimic the T Ψ C loops of tRNA, which have a much higher rate than that for the unstructured probes. This implies that ALKBH1 has a high preference for the stem-loop structure. The authors performed

steady-state kinetics of the ALKBH1-catalyzed demethylation of m1A in the stem-loop structured RNA and unstructured RNA probes. Both ALKBH1 kinetic and other substrate studies indicate that ALKBH1 may prefer bulged DNA or stem-loops of tRNAs over ss- and ds-DNA/RNA.

2.2. ALKBH2

ALKBH2 shares the most similar substrate preference with AlkB and is classified as a bona fide DNA repair enzyme together with ALKBH3. ALKBH2 performs demethylation more efficiently on ds-DNA than ss-DNA, while ALKBH3, also an active DNA/RNA demethylase, prefers ss-DNA [11]. Structure analysis of ALKBH2 shows that it uses a finger residue to search for and flip the damaged base into the active site; this specific binding mode ensures the lesion is repaired [92]. The divergent F1 β -hairpins in the vicinity of the active sites of ALKBH2 and ALKBH3 are important for their selectivity: after switching the F1 sites between both proteins, their activities also switched [93]. Similar results were obtained for swapping the ss- or ds-DNA preference of ALKBH2 and ALKBH3 by changing the relevant binding motifs [94].

Major substrates for ALKBH2 are m3C and m1A [11,31], together with other minor substrates, such as m3T [22] and m1G [95]. m5C can be oxidized by ALKBH2 [96]. Exocyclic etheno lesions ϵ A, ϵ C, 1,N²- ϵ G [56] are also repaired by ALKBH2. ALKBH2 is reported to repair N³-ethylthymine [97] and 1-ethyladenine. Since m1A and m3C DNA lesions exist in our body and ALKBH2 repairs them most effectively among all the substrates, ALKBH2 repair of these two substrates has been intensively studied for the kinetic behavior of these reactions. The reaction mechanism of AlkBH2 has also been studied computationally using QM/MM and MD methods [20]. Importantly, these studies revealed an influence of the ds-DNA on flexibility, enzyme dynamics and long-range correlated motions in the reaction pathway.

m1A. The kinetic studies of m1A were completed using DNA and 2-OG as substrates (Table 2) [61]. The results with 2-OG as co-substrate demonstrate that ALKBH2 repairs m1A in ds-DNA ($k_{\text{cat}}/K_m = 0.34 \text{ min}^{-1} \mu\text{M}^{-1}$) faster than ss-m1A ($k_{\text{cat}}/K_m = 0.27 \text{ min}^{-1} \mu\text{M}^{-1}$). Similarly, when using DNA as substrate, ALKBH2 can repair m1A in ds-DNA ($k_{\text{cat}}/K_m = 0.74 \text{ min}^{-1} \mu\text{M}^{-1}$) more efficiently than ss-m1A ($k_{\text{cat}}/K_m = 0.25 \text{ min}^{-1} \mu\text{M}^{-1}$) [61]. Furthermore, ALKBH2 is at least twice as efficient at removing m1A and m3C from ds-DNA [m1A ($k_{\text{cat}}/K_m = 2572.5 \text{ min}^{-1} \mu\text{M}^{-1}$) and m3C ($k_{\text{cat}}/K_m = 3176.0 \text{ min}^{-1} \mu\text{M}^{-1}$)] compared to single-stranded DNA [m1A ($k_{\text{cat}}/K_m = 1082.0 \text{ min}^{-1} \mu\text{M}^{-1}$) and m3C ($k_{\text{cat}}/K_m = 773.7 \text{ min}^{-1} \mu\text{M}^{-1}$)]. Kinetic studies were also performed on a novel methylation-sensitive nucleic acid (RNA) probe of m1A [CGCGm1AAUUCGCG ($k_{\text{cat}}/K_m = 3.4 \text{ min}^{-1} \mu\text{M}^{-1}$)] [60], which switches conformation according to its methylation status. Combined with differential scanning fluorimetry measurements, this enables highly sensitive and selective detection of demethylase activity at a single methylated base level. As a result of the CGCGm1AAUUCGCG self-complementary nature, it can inherently adopt a bi-molecular duplex through intermolecular base pairing and a monomolecular hairpin by intramolecular pairing. In comparison, ALKBH2 kinetic properties on regular sequences [ss-RNA ($k_{\text{cat}}/K_m = 4.30 \text{ min}^{-1} \mu\text{M}^{-1}$) and ds-RNA ($k_{\text{cat}}/K_m = 7.4 \text{ min}^{-1} \mu\text{M}^{-1}$)] were also reported [60].

m3C. For the previously mentioned m1A kinetic studies, similar experiments were also performed on m3C [61]. The kinetic parameter for ALKBH2 repairing m3C with 2-OG as co-substrate is $k_{\text{cat}}/K_m = 1.3 \text{ min}^{-1} \mu\text{M}^{-1}$ for ds-DNA, which is also better than the repair of ss-m3C ($k_{\text{cat}}/K_m = 1.2 \text{ min}^{-1} \mu\text{M}^{-1}$). When DNA is used as substrate, ALKBH2 repairing m3C also prefers m3C in ds-DNA ($k_{\text{cat}}/K_m = 1.10 \text{ min}^{-1} \mu\text{M}^{-1}$) over ss-m3C ($k_{\text{cat}}/K_m = 0.53 \text{ min}^{-1} \mu\text{M}^{-1}$) Lee et al. [61] reported that ALKBH2 is much more efficient at removing m3C in ds-DNA ($k_{\text{cat}}/K_m = 3176.0 \text{ min}^{-1} \mu\text{M}^{-1}$) compared to ss-DNA ($k_{\text{cat}}/K_m = 773.7 \text{ min}^{-1} \mu\text{M}^{-1}$) [59]. Theoretical studies delineated the reaction mechanism of AlkBH2 with ss-DNA and ds-DNA containing m3C and revealed the key interactions involved in the catalysis [20].

2.3. ALKBH3

ALKBH3, another well-studied AlkB homolog, has been found to actively demethylate m1A and m3C in DNA/RNA, and the protein prefers ss-DNA substrates [11]. The crystal structure of ALKBH3 [98] shows a flexible hairpin involved in flip nucleotide binding and discrimination of ss/ds-DNA [93]. ALKBH3 can repair other minor substrates such as m3T and m5C in ss/ds DNA [22,95,96]. ALKBH3 also repairs ϵ C [56], ϵ A [26], 3-ethylthymine [97] and 1-ethyladenine [31].

Kinetic studies of ALKBH3 are often performed in parallel with ALKBH2. For example, ALKBH3 repairs ss-DNA m1A ($k_{\text{cat}}/K_m = 982.4 \text{ min}^{-1} \mu\text{M}^{-1}$) and m3C ($k_{\text{cat}}/K_m = 763.0 \text{ min}^{-1} \mu\text{M}^{-1}$) [59]. Because 2-OG, nucleic acid modification, and molecular oxygen are the co-substrates of the 2-OG/Fe(II)-dependent reactions, every one of them could be used as a variable substrate for a kinetic study. For using 2-OG as co-substrate, ALKBH3 repairs ss-m1A ($k_{\text{cat}}/K_m = 0.51 \text{ min}^{-1} \mu\text{M}^{-1}$) and ss-m3C ($k_{\text{cat}}/K_m = 0.87 \text{ min}^{-1} \mu\text{M}^{-1}$); while using DNA as substrate, ALKBH3 repairs ss-m1A ($k_{\text{cat}}/K_m = 0.52 \text{ min}^{-1} \mu\text{M}^{-1}$) and ss-m3C ($k_{\text{cat}}/K_m = 1.03 \text{ min}^{-1} \mu\text{M}^{-1}$) [61].

Researchers revealed that ALKBH3 repairs m1A in ss-RNA ($k_{\text{cat}}/K_m = 3.13 \text{ min}^{-1} \mu\text{M}^{-1}$) [62]. ALKBH3 also repairs ss-m1A in RNA ($k_{\text{cat}}/K_m = 3.18 \text{ min}^{-1} \mu\text{M}^{-1}$), m1A in ds-RNA ($k_{\text{cat}}/K_m = 0.39 \text{ min}^{-1} \mu\text{M}^{-1}$), and m1A-probe in RNA ($k_{\text{cat}}/K_m = 2.1 \text{ min}^{-1} \mu\text{M}^{-1}$) [60]. ALKBH3 can promote cancer progression through demethylating m1A in tRNA, which is more easily cleaved by the protein angiogenin into tRNA-derived small RNAs when demethylated. The following binding of the fragments to Cytochrome *c* prevents apoptosis [99]. ALKBH3 catalyzes demethylation of m1A and m3C in tRNA. Michaelis–Menten steady-state kinetic studies of ALKBH3 have been performed in the stem-loop structure of RNA probes that mimic T Ψ C loops of tRNA. The results show that ALKBH3 quickly demethylates m1A and m3C of tRNA in vitro, which is similar to the m1A demethylation activity of ALKBH1 [91]. ALKBH3 can bind with ASCC3, which is the biggest subunit of ASCC (activating signal cointegrator complex), which can counter alkylation damage [100], and ALKBH-mediated DNA dealkylation repair has shown improved kinetics after binding [101].

2.4. ALKBH5

ALKBH5 proteins are partially localized in nuclear speckles and have been shown to function as an m6A RNA demethylase besides FTO [64]. m6A modifications are notably distributed within the RR(m6A)CU consensus motif, where R represents G or A [102,103]. ALKBH5 also has been reported to repair N⁶,N⁶-dimethyladenine [104]. Kinetic studies show that ALKBH5 demethylates m6A ($k_{\text{cat}}/K_m = 0.12 \text{ min}^{-1} \mu\text{M}^{-1}$) [64]. ALKBH5 has been correlated to FTO since they operate on the same substrate m6A in RNA. FTO and ALKBH5 have been reported to be strongly transcript-specific. Demethylation for different sequences can range from 1% to 46% for ALKBH5 catalyzed demethylation of m6A, where the sequence-containing consensus motif demonstrated high activity. Note that duplex-hairpin structures of the substrate can significantly decrease activity. Four sequences were selected to perform further steady-state kinetic studies ($k_{\text{cat}}/K_m = 0.053$ to $0.098 \text{ min}^{-1} \mu\text{M}^{-1}$) [67]. It has been reported that ALKBH5 demethylates m6A in ss-RNA, yielding $K_m = 0.192 \mu\text{M}$, and $k_{\text{cat}}/K_m = 0.12 \text{ min}^{-1} \mu\text{M}^{-1}$ was obtained with 2-OG as co-substrate [66]. One kinetic study investigated m6A repair by ALKBH5 in ss-RNA, while also considering the effect of NADP and its various forms on facilitating demethylation. However, there is no evidence that NADP can enhance ALKBH5 activity. The kinetic value of ALKBH5 repair of m6A is $k_{\text{cat}}/K_m = 0.23 \text{ min}^{-1} \mu\text{M}^{-1}$ [68]. Another kinetic study of ALKBH5 repair of m6A obtained $k_{\text{cat}}/K_m = 0.11 \text{ min}^{-1} \mu\text{M}^{-1}$ [65]. In the same kinetic experiment mentioned in the ALKBH3 part, they also tested ALKBH5 kinetic parameters, and the results show that ALKBH5 repairs m6A ($k_{\text{cat}}/K_m = 0.098 \text{ min}^{-1} \mu\text{M}^{-1}$) [62]. Furthermore, the activity of ALKBH5 on m6A was measured when researchers pursued different fusion tags to increase heterologous expression and solubility of ALKBH5 within *E. coli* [69]. A novel fusion tag EIN (the N-terminal domain of bacterial enzyme 1) was applied for

recombinant expression of the human RNA demethylases ALKBH5 and FTO. The tag dramatically increased the solubility of the protein and was easily removed by proteases. A kinetic study was performed to evidence that the enzymes were active. These ALKBH5 proteins demethylate m6A ($k_{\text{cat}}/K_m = 1.6 \text{ min}^{-1} \mu\text{M}^{-1}$) [69]. Most recently, two selective, novel inhibitors were found for ALKBH5, and the authors also tested the kinetics of m6A demethylation by using 2-OG as co-substrate ($k_{\text{cat}}/K_m = 18.57 \text{ min}^{-1} \mu\text{M}^{-1}$) [105].

2.5. FTO

FTO is a protein that was associated with human obesity through a gene-finding strategy [106]. It was later determined that FTO is an 2-OG dependent dioxygenase that can repair m3T and 3-methyluracil [72,107]. FTO was also reported to demethylate m6A, which is partially localized in nuclear speckles [33]. Later, FTO has been reported to repair m6A_m better than m6A kinetically [70]. Most recently, FTO was found to repair m1A and m3C in tRNA [108].

The oxidation of m6A by FTO generates N⁶-hydroxymethyladenosine (hm6A) and N⁶-formyladenosine (f6A) intermediates [109]. Although FTO and ALKBH5 share similar conserved active sites [110], it has been reported that ALKBH5 does not generate these intermediates. Computational studies demonstrated how conformational dynamics influences the substrate binding [111] and catalytic mechanism of FTO [112].

3-Methyluracil and 3-methylthymine. FTO was shown to catalyze the demethylation of m3U in ss-RNA ($k_{\text{cat}}/K_m = 0.014 \times 10^3 \text{ min}^{-1} \mu\text{M}^{-1}$) with higher efficiency than m3T in ss-DNA ($k_{\text{cat}}/K_m = 0.007 \times 10^3 \text{ min}^{-1} \mu\text{M}^{-1}$) [72]. 2-OG was also identified as a co-substrate for FTO repair of m3U in an effort to determine whether FTO is a sensor for 2-OG levels. The authors used a stem-loop substrate containing m3U with FAM (6-carboxyfluorescein), which can be cleaved by RNase after the demethylation of m3U to uracil. The K_m of 2-OG was found to be 2.88 μM , which is 10-fold lower than the estimated intracellular condition. The result shows that FTO is unlikely to be a sensor for 2-OG [71].

N⁶,2'-O-dimethyladenosine. The kinetics of FTO demethylating m6A_m were studied for m6A_m adjacent to the m7G cap. mRNA can be methylated at the 2'-hydroxyl position of the ribose sugar [113]. If the nucleotide followed by m7G with a triphosphate link at 5' end of mRNAs is 2'-O-methyladenosine (A_m), it can be methylated further into m6A_m [114]. FTO can demethylate m6A_m with $k_{\text{cat}}/K_m = 6.55 \text{ min}^{-1} \mu\text{M}^{-1}$ [70].

N⁶-methyladenine. FTO as an RNA demethylase has efficient oxidative demethylation activity targeting the m6A residues in RNA in vitro ($k_{\text{cat}}/K_m = 0.724 \text{ min}^{-1} \mu\text{M}^{-1}$) [33]. NADP has been shown to strongly bind to FTO and enhance FTO-mediated m6A demethylation in vitro and in vivo. Different forms of NADP derivatives and cofactor vitamin C have been added to the reaction mixture, exhibiting different capabilities to increase FTO activity, implying that FTO is potentially involved in the regulation of the cellular redox state [68]. The authors also found that NADP exerts much less effect on ALKBH5 than FTO, implying distinct regulatory mechanisms for ALKBH5 and FTO. For FTO demethylation of m6A in ss-RNA, the kinetic parameters were reported in the presence of 50 μM cofactors, NADP ($k_{\text{cat}}/K_m = 1.01 \text{ min}^{-1} \mu\text{M}^{-1}$), NADH ($k_{\text{cat}}/K_m = 0.55 \text{ min}^{-1} \mu\text{M}^{-1}$), NADP⁺ ($k_{\text{cat}}/K_m = 0.29 \text{ min}^{-1} \mu\text{M}^{-1}$), NAD⁺ ($k_{\text{cat}}/K_m = 0.20 \text{ min}^{-1} \mu\text{M}^{-1}$), and vitamin C ($k_{\text{cat}}/K_m = 0.045 \text{ min}^{-1} \mu\text{M}^{-1}$) [68]. For comparison, FTO repairs m6A under regular conditions (2 mM vitamin C) with $k_{\text{cat}}/K_m = 0.78 \text{ min}^{-1} \mu\text{M}^{-1}$ [68]. As mentioned above in the ALKBH5 section, m6A modifications are typically allocated within the RR(m6A)CU consensus motif. Sequence-dependent kinetic measurements were also performed for FTO demethylation of m6A; here, demethylation activities for various sequences range from 2% to 78%. Four sequences were selected to run further steady-state kinetic studies, and their kinetic data range is 0.39 to 0.77 $\text{min}^{-1} \mu\text{M}^{-1}$ for k_{cat}/K_m [67]. In the previously mentioned tags fusion study, FTO demethylation of m6A was also measured for its kinetic parameters: untagged FTO demethylates m6A with $k_{\text{cat}}/K_m = 0.69 \text{ min}^{-1} \mu\text{M}^{-1}$ [62]. Other FTO oxidizing m6A abilities were also tested: $k_{\text{cat}}/K_m = 0.0013 \text{ min}^{-1} \mu\text{M}^{-1}$ [69] and $k_{\text{cat}}/K_m = 0.63 \text{ min}^{-1} \mu\text{M}^{-1}$ [65]. Researchers also found that FTO demethylates regular

m6A at the GGm6ACU consensus motif ($k_{\text{cat}}/K_m = 0.06 \text{ min}^{-1} \mu\text{M}^{-1}$) and m6A next to the m7G triphosphate cap ($k_{\text{cat}}/K_m = 0.07 \text{ min}^{-1} \mu\text{M}^{-1}$) [70].

2.6. Ten-Eleven Translocation and J-Binding Protein (TET/JBP) Proteins

The first characterized TET/JBP family is JBP. It can catalyze the hydroxylation of thymine in DNA into hm5U as the first step of synthesizing base J [115,116]. It is found in the kinetoplastid flagellates, such as pathogenic *Trypanosoma* and *Leishmania* species [117,118], but is absent from eukaryotes, prokaryotes, and viruses [43].

TET proteins (TET1, TET2, and TET3) are identified as mammalian homologs of the trypanosome protein JBP [35]. Experiments show that TET proteins are 2-OG dependent enzymes that successively oxidize 5-methylcytosine into 5-hydroxymethylcytosine, 5-formylcytosine and 5-carboxylcytosine [34]. TET2 has been studied for its kinetic activity. The results show that TET2 is more active on m5C ($k_{\text{cat}}/K_m = 0.27 \text{ min}^{-1} \mu\text{M}^{-1}$) than hm5C ($k_{\text{cat}}/K_m = 0.042 \text{ min}^{-1} \mu\text{M}^{-1}$) and f5C ($k_{\text{cat}}/K_m = 0.021 \text{ min}^{-1} \mu\text{M}^{-1}$). hm5C is less prone to be further oxidized than m5C, suggesting that hm5C could be a potential stable biomarker for regulatory functions [63]. Until now, there has been no report on the kinetic properties of TET1 and 3. Computational studies elaborated on the catalytic mechanism of TET2 and the effects of clinically important mutations on the reaction mechanism as well as its reaction with unnatural alkylated substrates [119–122].

2.7. AlkB

AlkB is one of four enzymes in *E. coli* that respond to alkylation damage during the adaptive response [123]. The AlkB structure [74] shows that this enzyme uses a base-flipping mechanism to detect the damaged base [92]. Various substrates of AlkB have been reported and studied [44,124]. Computational studies revealed the catalytic mechanism of AlkB with a variety of alkylated substrates [20,125–128]. Importantly, studies reveal the effects of the nature of the substrate (ss- vs. ds-DNA) and the influence of long-range interactions and enzyme and substrate dynamics on the reaction mechanism [20].

1-Methyladenine. m1A and m3C were found to be the major substrates of AlkB. The kinetic study of AlkB repair of m1A was first performed using various substrates: minimal and extended substrate, poly(dA) containing m1A, short DNA oligonucleotides, and nucleotide triphosphate [73]. The authors found that long DNA substrates have better activity than short oligonucleotides. The minimal substrate for AlkB is 1-me-dAMP(5') ($k_{\text{cat}}/K_m = 0.80 \text{ min}^{-1} \mu\text{M}^{-1}$), while the trimer dTm1AT has a high kinetic value ($k_{\text{cat}}/K_m = 2.6 \text{ min}^{-1} \mu\text{M}^{-1}$). In addition, substrates lacking a phosphate at the 5' position to the lesion are poor substrates for demethylation: compare 1-me-dAMP (3') ($k_{\text{cat}}/K_m = 0.2 \text{ min}^{-1} \mu\text{M}^{-1}$) to 1-me-dAMP (5') ($k_{\text{cat}}/K_m = 2.1 \text{ min}^{-1} \mu\text{M}^{-1}$) [73]. Later, another study tested m1A demethylation with the same trimer sequence, dTm1AT, and obtained similar results ($k_{\text{cat}}/K_m = 3.7 \text{ min}^{-1} \mu\text{M}^{-1}$) [74]. Another study used formaldehyde dehydrogenase to convert the byproduct formaldehyde to formic acid and monitor the generation of an NADH analog using fluorescence. The results show that AlkB demethylates ds-1mA ($k_{\text{cat}}/K_m = 0.48 \text{ min}^{-1} \mu\text{M}^{-1}$) and ss-m1A ($k_{\text{cat}}/K_m = 0.68 \text{ min}^{-1} \mu\text{M}^{-1}$) with comparable efficiencies, and that the enzyme only has a modest preference for ss-DNA substrates [75]. In these experiments, differences in nucleic acid substrate length, the binding of diverse substrates, and coupling between successive chemical steps in the reaction cycle could account for the varying results, indicating that accessory factors could potentially influence the recognition of damaged bases in vivo. AlkB protein repairs the trimer Tm1AT ($k_{\text{cat}}/K_m = 1.9 \text{ min}^{-1} \mu\text{M}^{-1}$) much less efficiently compared to the pentamer Cam1AAT ($k_{\text{cat}}/K_m = 97.0 \text{ min}^{-1} \mu\text{M}^{-1}$) [76]. A kinetic study was performed investigating the dynamic conformational transitions of AlkB. The authors found that the key conformational transition controlling the catalytic cycle of AlkB involves movement of the nucleotide recognition lid that interacts with the Fe(II)/2-OG core. Their results show that AlkB repairs m1A with $k_{\text{cat}}/K_m = 0.68 \text{ min}^{-1} \mu\text{M}^{-1}$ [77]. Moreover, active site residues were identified and mutated and the results show different demethylation activities: $k_{\text{cat}}/K_m = 3.7 \text{ min}^{-1}$

μM^{-1} for unmodified AlkB repairing m1A in DNA, $k_{\text{cat}}/K_{\text{m}} = 1.6 \text{ min}^{-1} \mu\text{M}^{-1}$ for repair in RNA, $k_{\text{cat}}/K_{\text{m}} = 0.018 \text{ min}^{-1} \mu\text{M}^{-1}$ for AlkB D135N, $k_{\text{cat}}/K_{\text{m}} = 0.030 \text{ min}^{-1} \mu\text{M}^{-1}$ for AlkB E136L, and $k_{\text{cat}}/K_{\text{m}} = 0.035 \text{ min}^{-1} \mu\text{M}^{-1}$ for AlkB D135L [65]. In the previously mentioned self-complementary probe using the scanning fluorimetry technique to study ALKBH2, the authors also tested m1A repair by AlkB and found $k_{\text{cat}}/K_{\text{m}} = 0.63 \text{ min}^{-1} \mu\text{M}^{-1}$; ss-m1A repair in RNA gave $k_{\text{cat}}/K_{\text{m}} = 2.6 \text{ min}^{-1} \mu\text{M}^{-1}$; and m1A in ds-DNA repair in RNA gave $k_{\text{cat}}/K_{\text{m}} = 3.2 \text{ min}^{-1} \mu\text{M}^{-1}$ [60]. For AlkB repair of ss-m1A, $k_{\text{cat}}/K_{\text{m}} = 0.59 \text{ min}^{-1} \mu\text{M}^{-1}$ was found; and for m1A in ds-DNA, $k_{\text{cat}}/K_{\text{m}} = 0.38 \text{ min}^{-1} \mu\text{M}^{-1}$ was determined [61]. Recently, Baldwin et al. used a transient-state kinetic analysis for single turnover reactions to determine the elementary steps of the enzymatic mechanism. Their kinetic data show a faster rate than previously reported. In short, this method requires rapid mixing of a substrate with sufficient enzyme to directly observe intermediates and products formed in one single reaction cycle. The advantage of this method is that it avoids the problem of self-inactivation of dioxygenases during multiple turnovers. The transient-state kinetics analysis also shows that AlkB can repair m1A preferentially in single-stranded DNA ($k_{\text{cat}}/K_{\text{m}} = 1317.1 \text{ min}^{-1} \mu\text{M}^{-1}$) over double-strand DNA ($k_{\text{cat}}/K_{\text{m}} = 71.1 \text{ min}^{-1} \mu\text{M}^{-1}$) [78].

3-Methylcytosine. m3C was also tested by the method of formaldehyde dehydrogenase converting formaldehyde to formic acid and monitoring the generation of an NADH analog using fluorescence. The results show that AlkB demethylates m3C in ds-DNA ($k_{\text{cat}}/K_{\text{m}} = 0.35 \text{ min}^{-1} \mu\text{M}^{-1}$) and ss-m3C ($k_{\text{cat}}/K_{\text{m}} = 0.65 \text{ min}^{-1} \mu\text{M}^{-1}$) [75]. Other studies used an approach to directly quantitate DNA substrates and products that differ by a single methyl group, based on capillary electrophoresis with laser-induced fluorescence detection. This study achieved baseline separation of a 15mer nucleotide with a fluorescence label and a single m3C unit and obtained $k_{\text{cat}}/K_{\text{m}} = 73.6 \text{ min}^{-1} \mu\text{M}^{-1}$ [80]. In the study on the dynamic conformational transitions of AlkB, similar kinetic results were obtained for AlkB repair of m3C ($k_{\text{cat}}/K_{\text{m}} = 53.0 \text{ min}^{-1} \mu\text{M}^{-1}$) [77]. AlkB kinetic parameters for repairing m3C in ss-DNA ($k_{\text{cat}}/K_{\text{m}} = 1.2 \text{ min}^{-1} \mu\text{M}^{-1}$) and ds-DNA ($k_{\text{cat}}/K_{\text{m}} = 0.76 \text{ min}^{-1} \mu\text{M}^{-1}$) were also reported [61]. Nigam et al. found that AlkB inefficiently repairs m3C in long ss-DNA but readily repairs single-strand DNA binding protein (SSB)-bound methylated ss-DNA of equal length. The 70mer poly T was used as the DNA sequence, with m3C present in different positions in the sequence, and their AlkB efficiency was tested with SSB. m3C at position 15 shows the highest activity ($K_{\text{m}} = 8.2 \mu\text{M}^{-1}$) over the m3C at position 1 ($K_{\text{m}} = 2.4 \mu\text{M}^{-1}$), a location that could potentially be wrapped by SSB [81].

1,N⁶-ethenoadenine. ϵA is one of the etheno-DNA lesions, which are exocyclic DNA lesions usually formed by exposure to either lipid peroxidation (LPO) products or the carcinogen vinyl chloride [56]. It is repaired by direct reversal repair (AlkB) and base excision repair (AAG, alkyladenine DNA glycosylase). The repair of ϵA by AlkB was initially reported in 2005 [25,26].

Kinetic studies of AlkB repairing ϵA have also been carried out by different laboratories with various methods. Yu et al. performed a kinetic study of AlkB repairing the T ϵ AT trimer and found $k_{\text{cat}}/K_{\text{m}} = 0.0020 \text{ min}^{-1} \mu\text{M}^{-1}$ [76]. Gururaj et al. detected glyoxal, a byproduct of ϵA repair, by reaction with 2-hydrazinobenzothiazole, forming a yellow-colored compound with a distinct absorption spectrum with an absorption band at 365 nm. Their results show that a 40mer containing adenine, treated by chloroacetaldehyde to form ϵA , is repaired by AlkB with $k_{\text{cat}}/K_{\text{m}} = 0.0019 \text{ min}^{-1} \mu\text{M}^{-1}$ [82]. As mentioned in the above section of m1A, a transient state kinetic study shows that AlkB can repair ϵA in ss-DNA ($k_{\text{cat}}/K_{\text{m}} = 8.5 \text{ min}^{-1} \mu\text{M}^{-1}$) and ds-DNA ($k_{\text{cat}}/K_{\text{m}} = 12.1 \text{ min}^{-1} \mu\text{M}^{-1}$) [78].

N⁶-methyladenine. AlkB has a relatively low activity to m6A compared to m1A and m3C. Zhu et al. performed kinetic studies of m6A repair by wild-type and mutant AlkB. The unmodified AlkB shows $k_{\text{cat}}/K_{\text{m}} = 0.007 \text{ min}^{-1} \mu\text{M}^{-1}$, whereas the AlkB variants having swapped sequences from FTO and ALKBH5 show improved activity towards m6A [65].

N1-methylguanine. AlkB has been reported to repair m1G with weak activity. The Pan group identified the AlkB D135S variant, which has higher reactivity than the wild-type enzyme for repairing m1G. Aspartic acid 135 has been reported to be able to form H-bonds with the N6 group of adenine and cytidine [74]. A high throughput platform was used to evaluate variants of AlkB. AlkB variant D135T has the highest activity toward m1G ($k_{\text{cat}}/K_{\text{m}} = 15.7 \pm 3.7 \text{ min}^{-1} \mu\text{M}^{-1}$) [79]. The results reveal that these positively charged substrates are favorably positioned in the active site by interacting with the negatively charged carboxylate group of D135; the shorter side chain of D135S seems to allow more room to accommodate m1G while sustaining the crucial hydrogen bond with m1G, which may explain the improvement in activity. The engineered variant of AlkB D135V/L118V can convert N^2,N^2 -dimethylguanosine (m22G) into m2G [129].

2.8. Other Mammalian Homologs of AlkB

ALKBH4, ALKBH7, and ALKBH8 have been tested with respect to their demethylation activities. ALKBH4 demethylates m6A in DNA; it can also mediate the demethylation of a monomethylated site in actin (K84me1), which controls the actin–myosin interaction and other actomyosin-dependent processes, such as cytokinesis and cell migration [130]. ALKBH6 in humans is localized in the nucleus and cytoplasm; the substrate of ALKBH6 has yet to be discovered [131,132]. ALKBH7 is nuclear-encoded but is primarily localized in the mitochondria of mammalian cells. ALKBH7 demethylates m22G and m1A within mitochondrial Ile and Leu1 pre-tRNA regions [133]. ALKBH7 has also been reported to repair ϵ A [134]. ALKBH8 is exclusively located in the cytoplasm and has three domains: the N-terminal RNA recognition motif, the middle 2-OG/Fe(II)-dependent AlkB-like domain, and the C-terminal methyltransferase domain. Its structure and hydroxylation of 5-methoxycarbonylmethyluridine (mcm5U) suggest a potential role in the regulation of posttranscriptional tRNA modification through methylation/demethylation [135].

3. Conclusions

In this review, we inspect the AlkB and TET family proteins, mainly focusing on their kinetic behaviors. Many researchers have shown that these enzymes demethylate various substrates in DNA and RNA. Kinetic studies have provided important information with respect to the mechanism of an enzyme-catalyzed reaction by determining the rate of reaction and how the rate changes in response to changes in experimental parameters. Among the kinetic parameters, the ratio of $k_{\text{cat}}/K_{\text{m}}$ provides a reliable measure of catalytic efficiency.

A useful application of kinetic studies is to compare repair efficiency of different DNA/RNA substrates (modified bases). Some examples are listed below. Studies show that ALKBH2 and ALKBH3 prefer repairing m1A/m3C over m3T/m1G, and ALKBH3 prefers to repair lesions in ss-DNA/RNA, while ALKBH2 prefers to repair lesions in ds-DNA [95]. There is more information from the kinetic studies that can further help us understand the reaction mechanism. For instance, FTO was first discovered to repair m3T and m3U, but the kinetic parameters are relatively low compared to other ALKBH family proteins [72,107]; later, m6A was discovered as a better substrate [33]. Kinetics is also a tool to find out about the property of a protein in vivo. In the case of NADPH modulating FTO, the results imply that FTO is involved in the regulation of the cellular redox state, while there is no such effect for ALKBH5 [68]. 2-OG was also measured as a substrate for FTO to repair the m3U lesion; the kinetic results show FTO is a sensor for cellular 2-OG levels [71]. TET2 is more efficient in oxidizing m5C than hm5C, suggesting that TET2 is possibly evolutionarily tuned and hm5C is a potential stable marker with regulatory functions [63]. Kinetics also show the sequence-dependent activities of enzymes, such that ALKBH5 and FTO prefer the GG(m6A)CU consensus sequence. In addition, substrates in duplex-hairpin structures significantly decrease enzyme activity [67].

In most kinetic studies, the conversion of an enzymatic reaction is usually lower than 20% to obtain accurate kinetic parameters. For the detection of starting material and product, many studies use LC-MS, because a repaired base usually has less MW than the starting

material. HPLC with a UV detector has been widely used for detection as well, because DNA bases have strong absorbances around 260 nm in the UV spectrum, and the starting material and the product can be separated by different types of columns [136]. Sometimes it is hard to detect the amount of product DNA; in such cases, researchers have used other co-products, for example formaldehyde and glyoxal (Figure 1), to monitor the reactions. A research group used formaldehyde dehydrogenase to convert formaldehyde to formic acid and monitored the formation of an NADH analog using fluorescence [75]. Gururaj et al. used glyoxal, a byproduct of ϵ A repair, and reacted it with 2-hydrazinobenzothiazole, which forms a complex with a yellow color that has a distinct absorption spectrum with a band at 365 nm [82].

For an individual enzyme, there could be several DNA/RNA substrates. How to differentiate the repair efficiency among them needs a kinetic study carried out under the same condition for all substrates. In the literature, different methods provide different kinetic parameters even for the same enzyme and substrate. The data from different sources may not be able to distinguish the differences between these substrates. For example, it was initially reported that ALKBH2 repairs m1A in ds-DNA with $k_{\text{cat}}/K_m = 2572.5 \text{ min}^{-1} \mu\text{M}^{-1}$ and m3C with $k_{\text{cat}}/K_m = 3176 \text{ min}^{-1} \mu\text{M}^{-1}$, compared to m1A in single-stranded DNA ($k_{\text{cat}}/K_m = 1100 \text{ min}^{-1} \mu\text{M}^{-1}$) and m3C in ss-DNA ($k_{\text{cat}}/K_m = 775 \text{ min}^{-1} \mu\text{M}^{-1}$) [59]. These numbers are quite different from later published results: ALKBH2 repairs m1A in ds-DNA ($k_{\text{cat}}/K_m = 0.74 \text{ min}^{-1} \mu\text{M}^{-1}$) and ss-m1A ($k_{\text{cat}}/K_m = 0.25 \text{ min}^{-1} \mu\text{M}^{-1}$) [61]. These differences are possibly due to the fact that the earlier results were obtained by using restriction enzymes to cut the repaired oligomers for measuring the demethylation. Additionally, the reaction time course was monitored at a single time point, 1 h, which is typically long for kinetic studies. Single turnover reactions could generate kinetic data that are faster than data from steady-state kinetics [78]. These examples demonstrate the necessity of performing the kinetic studies of an enzyme with all of its substrates under the same condition. The 2-OG/Fe(II)-dependent enzymes discussed in this review are important in genetics and epigenetics [61]. However, many substrates of certain enzymes are still not clear, and additionally, in many cases kinetic data are not available. One of the future goals for this research field is to study the mechanism and kinetic behavior of these proteins in a more detailed manner, and then apply this information to determine their functions in biology and disease.

Funding: This work was supported by the National Institutes of Health under grant numbers R01 ES028865 (to D.L.).

Conflicts of Interest: The authors declare no competing financial interests.

References

1. Rydberg, B.; Lindahl, T. Nonenzymatic Methylation of DNA by the Intracellular Methyl Group Donor S-Adenosyl-L-Methionine Is a Potentially Mutagenic Reaction. *EMBO J.* **1982**, *1*, 211–216. [[CrossRef](#)] [[PubMed](#)]
2. Mathison, B.H.; Frame, S.R.; Bogdanffy, M.S. DNA Methylation, Cell Proliferation, and Histopathology in Rats Following Repeated Inhalation Exposure to Dimethyl Sulfate. *Inhal. Toxicol.* **2004**, *16*, 581–592. [[CrossRef](#)] [[PubMed](#)]
3. Stone, M.P.; Cho, Y.-J.; Huang, H.; Kim, H.-Y.; Kozekov, I.D.; Kozekova, A.; Wang, H.; Minko, I.G.; Lloyd, R.S.; Harris, T.M.; et al. Interstrand DNA Cross-Links Induced by α,β -Unsaturated Aldehydes Derived from Lipid Peroxidation and Environmental Sources. *Acc. Chem. Res.* **2008**, *41*, 793–804. [[CrossRef](#)]
4. Marnett, L. Endogenous DNA Damage and Mutation. *Trends Genet.* **2001**, *17*, 214–221. [[CrossRef](#)]
5. Bordin, D.L.; Lirussi, L.; Nilsen, H. Cellular Response to Endogenous DNA Damage: DNA Base Modifications in Gene Expression Regulation. *DNA Repair* **2021**, *99*, 103051. [[CrossRef](#)]
6. Barrows, L.R.; Magee, P.N. Nonenzymatic Methylation of DNA by S-Adenosylmethionine in Vitro. *Carcinogenesis* **1982**, *3*, 349–351. [[CrossRef](#)]
7. Sedgwick, B.; Lindahl, T. Recent Progress on the Ada Response for Inducible Repair of DNA Alkylation Damage. *Oncogene* **2002**, *21*, 8886–8894. [[CrossRef](#)] [[PubMed](#)]
8. Lindahl, T.; Sedgwick, B.; Sekiguchi, M.; Nakabeppu, Y. Regulation and Expression of the Adaptive Response to Alkylating Agents. *Annu. Rev. Biochem.* **1988**, *57*, 133–157. [[CrossRef](#)]
9. Mielecki, D.; Grzesiuk, E. Ada Response—A Strategy for Repair of Alkylated DNA in Bacteria. *FEMS Microbiol. Lett.* **2014**, *355*, 1–11. [[CrossRef](#)]

10. Mielecki, D.; Wrzesiński, M.; Grzesiuk, E. Inducible Repair of Alkylated DNA in Microorganisms. *Mutat. Res./Rev. Mutat. Res.* **2015**, *763*, 294–305. [[CrossRef](#)]
11. Aas, P.A.; Otterlei, M.; Falnes, P.Ø.; Vågbø, C.B.; Skorpen, F.; Akbari, M.; Sundheim, O.; Bjørås, M.; Slupphaug, G.; Seeberg, E.; et al. Human and Bacterial Oxidative Demethylases Repair Alkylation Damage in Both RNA and DNA. *Nature* **2003**, *421*, 859–863. [[CrossRef](#)] [[PubMed](#)]
12. Aravind, L.; Koonin, E.V. The DNA-Repair Protein AlkB, EGL-9, and Leprecan Define New Families of 2-Oxoglutarate- and Iron-Dependent Dioxygenases. *Genome Biol* **2001**, *2*, research0007.1. [[CrossRef](#)] [[PubMed](#)]
13. Falnes, P.Ø.; Johansen, R.F.; Seeberg, E. AlkB-Mediated Oxidative Demethylation Reverses DNA Damage in *Escherichia coli*. *Nature* **2002**, *419*, 178–182. [[CrossRef](#)] [[PubMed](#)]
14. Trewick, S.C.; Henshaw, T.F.; Hausinger, R.P.; Lindahl, T.; Sedgwick, B. Oxidative Demethylation by *Escherichia coli* AlkB Directly Reverts DNA Base Damage. *Nature* **2002**, *419*, 174–178. [[CrossRef](#)] [[PubMed](#)]
15. Clifton, I.J.; McDonough, M.A.; Ehrismann, D.; Kershaw, N.J.; Granatino, N.; Schofield, C.J. Structural Studies on 2-Oxoglutarate Oxygenases and Related Double-Stranded β -Helix Fold Proteins. *J. Inorg. Biochem.* **2006**, *100*, 644–669. [[CrossRef](#)]
16. Hausinger, R.P. Fe(II)/ α -Ketoglutarate-Dependent Hydroxylases and Related Enzymes. *Crit. Rev. Biochem. Mol. Biol.* **2004**, *39*, 21–68. [[CrossRef](#)] [[PubMed](#)]
17. Welford, R.W.D.; Kirkpatrick, J.M.; McNeill, L.A.; Puri, M.; Oldham, N.J.; Schofield, C.J. Incorporation of Oxygen into the Succinate Co-Product of Iron(II) and 2-Oxoglutarate Dependent Oxygenases from Bacteria, Plants and Humans. *FEBS Lett.* **2005**, *579*, 5170–5174. [[CrossRef](#)]
18. Hutton, J.J.; Kaplan, A.; Udenfriend, S. Conversion of the Amino Acid Sequence Gly-Pro-Pro in Protein to Gly-Pro-Hyp by Collagen Proline Hydroxylase. *Arch. Biochem. Biophys.* **1967**, *121*, 384–391. [[CrossRef](#)]
19. Islam, M.S.; Leissing, T.M.; Chowdhury, R.; Hopkinson, R.J.; Schofield, C.J. 2-Oxoglutarate-Dependent Oxygenases. *Annu. Rev. Biochem.* **2018**, *87*, 585–620. [[CrossRef](#)]
20. Waheed, S.O.; Ramanan, R.; Chaturvedi, S.S.; Lehnert, N.; Schofield, C.J.; Christov, C.Z.; Karabancheva-Christova, T.G. Role of Structural Dynamics in Selectivity and Mechanism of Non-Heme Fe(II) and 2-Oxoglutarate-Dependent Oxygenases Involved in DNA Repair. *ACS Cent. Sci.* **2020**, *6*, 795–814. [[CrossRef](#)]
21. Delaney, J.C.; Essigmann, J.M. Mutagenesis, Genotoxicity, and Repair of 1-Methyladenine, 3-Alkylcytosines, 1-Methylguanine, and 3-Methylthymine in AlkB *Escherichia coli*. *Proc. Natl. Acad. Sci. USA* **2004**, *101*, 14051–14056. [[CrossRef](#)] [[PubMed](#)]
22. Koivisto, P.; Robins, P.; Lindahl, T.; Sedgwick, B. Demethylation of 3-Methylthymine in DNA by Bacterial and Human DNA Dioxygenases. *J. Biol. Chem.* **2004**, *279*, 40470–40474. [[CrossRef](#)] [[PubMed](#)]
23. Li, D.; Fedeles, B.I.; Shrivastav, N.; Delaney, J.C.; Yang, X.; Wong, C.; Drennan, C.L.; Essigmann, J.M. Removal of N-Alkyl Modifications from N(2)-Alkylguanine and N(4)-Alkylcytosine in DNA by the Adaptive Response Protein AlkB. *Chem. Res. Toxicol.* **2013**, *26*, 1182–1187. [[CrossRef](#)] [[PubMed](#)]
24. Li, D.; Delaney, J.C.; Page, C.M.; Yang, X.; Chen, A.S.; Wong, C.; Drennan, C.L.; Essigmann, J.M. Exocyclic Carbons Adjacent to the N6 of Adenine Are Targets for Oxidation by the *Escherichia coli* Adaptive Response Protein AlkB. *J. Am. Chem. Soc.* **2012**, *134*, 8896–8901. [[CrossRef](#)]
25. Delaney, J.C.; Smeester, L.; Wong, C.; Frick, L.E.; Taghizadeh, K.; Wishnok, J.S.; Drennan, C.L.; Samson, L.D.; Essigmann, J.M. AlkB Reverses Etheno DNA Lesions Caused by Lipid Oxidation in Vitro and in Vivo. *Nat. Struct. Mol. Biol.* **2005**, *12*, 855–860. [[CrossRef](#)]
26. Mishina, Y.; Yang, C.-G.; He, C. Direct Repair of the Exocyclic DNA Adduct 1,N⁶-Ethenoadenine by the DNA Repair AlkB Proteins. *J. Am. Chem. Soc.* **2005**, *127*, 14594–14595. [[CrossRef](#)]
27. Maciejewska, A.M.; Poznański, J.; Kaczmarek, Z.; Krowisz, B.; Nieminiński, J.; Polkowska-Nowakowska, A.; Grzesiuk, E.; Kuśmierk, J.T. AlkB Dioxygenase Preferentially Repairs Protonated Substrates: Specificity Against Exocyclic Adducts and Molecular Mechanism of Action. *J. Biol. Chem.* **2013**, *288*, 432–441. [[CrossRef](#)]
28. Maciejewska, A.M.; Ruszel, K.P.; Nieminiński, J.; Lewicka, J.; Sokołowska, B.; Grzesiuk, E.; Kuśmierk, J.T. Chloroacetaldehyde-Induced Mutagenesis in *Escherichia coli*: The Role of AlkB Protein in Repair of 3,N4-Ethenocytosine and 3,N4- α -Hydroxyethanocytosine. *Mutat. Res./Fundam. Mol. Mech. Mutagen.* **2010**, *684*, 24–34. [[CrossRef](#)]
29. Kurowski, M.A.; Bhagwat, A.S.; Papaj, G.; Bujnicki, J.M. Phylogenomic Identification of Five New Human Homologs of the DNA Repair Enzyme AlkB. *BMC Genom.* **2003**, *4*, 48. [[CrossRef](#)]
30. Sanchez-Pulido, L.; Andrade-Navarro, M.A. The FTO (Fat Mass and Obesity Associated) Gene Codes for a Novel Member of the Non-Heme Dioxygenase Superfamily. *BMC Biochem.* **2007**, *8*, 23. [[CrossRef](#)]
31. Duncan, T.; Trewick, S.C.; Koivisto, P.; Bates, P.A.; Lindahl, T.; Sedgwick, B. Reversal of DNA Alkylation Damage by Two Human Dioxygenases. *Proc. Natl. Acad. Sci. USA* **2002**, *99*, 16660–16665. [[CrossRef](#)]
32. Loos, R.J.F.; Bouchard, C. FTO: The First Gene Contributing to Common Forms of Human Obesity. *Obes. Rev.* **2008**, *9*, 246–250. [[CrossRef](#)] [[PubMed](#)]
33. Jia, G.; Fu, Y.; Zhao, X.; Dai, Q.; Zheng, G.; Yang, Y.; Yi, C.; Lindahl, T.; Pan, T.; Yang, Y.-G.; et al. N6-Methyladenosine in Nuclear RNA Is a Major Substrate of the Obesity-Associated FTO. *Nat. Chem. Biol.* **2011**, *7*, 885–887. [[CrossRef](#)] [[PubMed](#)]
34. He, Y.-F.; Li, B.-Z.; Li, Z.; Liu, P.; Wang, Y.; Tang, Q.; Ding, J.; Jia, Y.; Chen, Z.; Li, L.; et al. Tet-Mediated Formation of 5-Carboxylcytosine and Its Excision by TDG in Mammalian DNA. *Science* **2011**, *333*, 1303–1307. [[CrossRef](#)] [[PubMed](#)]

35. Tahiliani, M.; Koh, K.P.; Shen, Y.; Pastor, W.A.; Bandukwala, H.; Brudno, Y.; Agarwal, S.; Iyer, L.M.; Liu, D.R.; Aravind, L.; et al. Conversion of 5-Methylcytosine to 5-Hydroxymethylcytosine in Mammalian DNA by MLL Partner TET1. *Science* **2009**, *324*, 930–935. [[CrossRef](#)]
36. Ito, S.; Shen, L.; Dai, Q.; Wu, S.C.; Collins, L.B.; Swenberg, J.A.; He, C.; Zhang, Y. Tet Proteins Can Convert 5-Methylcytosine to 5-Formylcytosine and 5-Carboxylcytosine. *Science* **2011**, *333*, 1300–1303. [[CrossRef](#)]
37. Crawford, D.J.; Liu, M.Y.; Nabel, C.S.; Cao, X.-J.; Garcia, B.A.; Kohli, R.M. Tet2 Catalyzes Stepwise 5-Methylcytosine Oxidation by an Iterative and *de Novo* Mechanism. *J. Am. Chem. Soc.* **2016**, *138*, 730–733. [[CrossRef](#)]
38. Tamanaha, E.; Guan, S.; Marks, K.; Saleh, L. Distributive Processing by the Iron(II)/ α -Ketoglutarate-Dependent Catalytic Domains of the TET Enzymes Is Consistent with Epigenetic Roles for Oxidized 5-Methylcytosine Bases. *J. Am. Chem. Soc.* **2016**, *138*, 9345–9348. [[CrossRef](#)]
39. Yu, M.; Hon, G.C.; Szulwach, K.E.; Song, C.-X.; Jin, P.; Ren, B.; He, C. Tet-Assisted Bisulfite Sequencing of 5-Hydroxymethylcytosine. *Nat. Protoc.* **2012**, *7*, 2159–2170. [[CrossRef](#)]
40. Zhang, L.; Chen, W.; Iyer, L.M.; Hu, J.; Wang, G.; Fu, Y.; Yu, M.; Dai, Q.; Aravind, L.; He, C. A TET Homologue Protein from *Coprinopsis Cinerea* (CcTET) That Biochemically Converts 5-Methylcytosine to 5-Hydroxymethylcytosine, 5-Formylcytosine, and 5-Carboxylcytosine. *J. Am. Chem. Soc.* **2014**, *136*, 4801–4804. [[CrossRef](#)]
41. Yu, Z.; Genest, P.-A.; ter Riet, B.; Sweeney, K.; DiPaolo, C.; Kieft, R.; Christodoulou, E.; Perrakis, A.; Simmons, J.M.; Hausinger, R.P.; et al. The Protein That Binds to DNA Base J in Trypanosomatids Has Features of a Thymidine Hydroxylase. *Nucleic Acids Res.* **2007**, *35*, 2107–2115. [[CrossRef](#)]
42. Cliffe, L.J.; Kieft, R.; Southern, T.; Birkeland, S.R.; Marshall, M.; Sweeney, K.; Sabatini, R. JBP1 and JBP2 Are Two Distinct Thymidine Hydroxylases Involved in J Biosynthesis in Genomic DNA of African Trypanosomes. *Nucleic Acids Res.* **2009**, *37*, 1452–1462. [[CrossRef](#)] [[PubMed](#)]
43. Borst, P.; Sabatini, R. Base J: Discovery, Biosynthesis, and Possible Functions. *Annu. Rev. Microbiol.* **2008**, *62*, 235–251. [[CrossRef](#)] [[PubMed](#)]
44. Fedeles, B.I.; Singh, V.; Delaney, J.C.; Li, D.; Essigmann, J.M. The AlkB Family of Fe(II)/ α -Ketoglutarate-Dependent Dioxygenases: Repairing Nucleic Acid Alkylation Damage and Beyond. *J. Biol. Chem.* **2015**, *290*, 20734–20742. [[CrossRef](#)]
45. Kuznetsov, N.A.; Kanazhevskaya, L.Y.; Fedorova, O.S. DNA Demethylation in the Processes of Repair and Epigenetic Regulation Performed by 2-Ketoglutarate-Dependent DNA Dioxygenases. *Int. J. Mol. Sci.* **2021**, *22*, 10540. [[CrossRef](#)]
46. Perry, G.S.; Das, M.; Woon, E.C.Y. Inhibition of AlkB Nucleic Acid Demethylases: Promising New Epigenetic Targets. *J. Med. Chem.* **2021**, *64*, 16974–17003. [[CrossRef](#)] [[PubMed](#)]
47. Alemu, E.A.; He, C.; Klungland, A. ALKBHs-Facilitated RNA Modifications and de-Modifications. *DNA Repair* **2016**, *44*, 87–91. [[CrossRef](#)] [[PubMed](#)]
48. Kanazhevskaya, L.Y.; Smyshlyaev, D.A.; Alekseeva, I.V.; Fedorova, O.S. Conformational Dynamics of Dioxygenase AlkB and DNA in the Course of Catalytically Active Enzyme–Substrate Complex Formation. *Russ. J. Bioorg. Chem.* **2019**, *45*, 630–640. [[CrossRef](#)]
49. Ma, L.; Lu, H.; Tian, Z.; Yang, M.; Ma, J.; Shang, G.; Liu, Y.; Xie, M.; Wang, G.; Wu, W.; et al. Structural Insights into the Interactions and Epigenetic Functions of Human Nucleic Acid Repair Protein ALKBH6. *J. Biol. Chem.* **2022**, *298*, 101671. [[CrossRef](#)]
50. Kanazhevskaya, L.Y.; Alekseeva, I.V.; Fedorova, O.S. A Single-Turnover Kinetic Study of DNA Demethylation Catalyzed by Fe(II)/ α -Ketoglutarate-Dependent Dioxygenase AlkB. *Molecules* **2019**, *24*, 4576. [[CrossRef](#)]
51. Klose, R.J.; Bird, A.P. Genomic DNA Methylation: The Mark and Its Mediators. *Trends Biochem. Sci.* **2006**, *31*, 89–97. [[CrossRef](#)] [[PubMed](#)]
52. Bird, A. DNA Methylation Patterns and Epigenetic Memory. *Genes Dev.* **2002**, *16*, 6–21. [[CrossRef](#)] [[PubMed](#)]
53. Kinde, B.; Gabel, H.W.; Gilbert, C.S.; Griffith, E.C.; Greenberg, M.E. Reading the Unique DNA Methylation Landscape of the Brain: Non-CpG Methylation, Hydroxymethylation, and MeCP2. *Proc. Natl. Acad. Sci. USA* **2015**, *112*, 6800–6806. [[CrossRef](#)]
54. Dubin, D.T.; Taylor, R.H. The Methylation State of Poly A-Containing Messenger RNA from Cultured Hamster Cells. *Nucleic Acids Res.* **1975**, *2*, 1653–1668. [[CrossRef](#)] [[PubMed](#)]
55. Bartsch, H.; Nair, J. New DNA-Based Biomarkers for Oxidative Stress and Cancer Chemoprevention Studies. *Eur. J. Cancer* **2000**, *36*, 1229–1234. [[CrossRef](#)] [[PubMed](#)]
56. Zdzalik, D.; Domańska, A.; Prorok, P.; Kosicki, K.; van den Born, E.; Falnes, P.Ø.; Rizzo, C.J.; Guengerich, F.P.; Tudek, B. Differential Repair of Etheno-DNA Adducts by Bacterial and Human AlkB Proteins. *DNA Repair* **2015**, *30*, 1–10. [[CrossRef](#)]
57. Nair, J.; Godschalk, R.W.; Nair, U.; Owen, R.W.; Hull, W.E.; Bartsch, H. Identification of 3, *N*⁴-Etheno-5-Methyl-2'-Deoxycytidine in Human DNA: A New Modified Nucleoside Which May Perturb Genome Methylation. *Chem. Res. Toxicol.* **2012**, *25*, 162–169. [[CrossRef](#)]
58. Zhang, M.; Yang, S.; Nelakanti, R.; Zhao, W.; Liu, G.; Li, Z.; Liu, X.; Wu, T.; Xiao, A.; Li, H. Mammalian ALKBH1 Serves as an *N*⁶-MA Demethylase of Unpairing DNA. *Cell Res.* **2020**, *30*, 197–210. [[CrossRef](#)] [[PubMed](#)]
59. Lee, D.-H.; Jin, S.-G.; Cai, S.; Chen, Y.; Pfeifer, G.P.; O'Connor, T.R. Repair of Methylation Damage in DNA and RNA by Mammalian AlkB Homologues. *J. Biol. Chem.* **2005**, *280*, 39448–39459. [[CrossRef](#)]
60. Yang, T.; Cheong, A.; Mai, X.; Zou, S.; Woon, E.C.Y. A Methylation-Switchable Conformational Probe for the Sensitive and Selective Detection of RNA Demethylase Activity. *Chem. Commun.* **2016**, *52*, 6181–6184. [[CrossRef](#)]

61. Chen, F.; Bian, K.; Tang, Q.; Fedeles, B.I.; Singh, V.; Humulock, Z.T.; Essigmann, J.M.; Li, D. Oncometabolites D- and L-2-Hydroxyglutarate Inhibit the AlkB Family DNA Repair Enzymes under Physiological Conditions. *Chem. Res. Toxicol.* **2017**, *30*, 1102–1110. [[CrossRef](#)] [[PubMed](#)]
62. Das, M.; Yang, T.; Dong, J.; Prasetya, F.; Xie, Y.; Wong, K.H.Q.; Cheong, A.; Woon, E.C.Y. Multiprotein Dynamic Combinatorial Chemistry: A Strategy for the Simultaneous Discovery of Subfamily-Selective Inhibitors for Nucleic Acid Demethylases FTO and ALKBH3. *Chem. Asian J.* **2018**, *13*, 2854–2867. [[CrossRef](#)] [[PubMed](#)]
63. Hu, L.; Lu, J.; Cheng, J.; Rao, Q.; Li, Z.; Hou, H.; Lou, Z.; Zhang, L.; Li, W.; Gong, W.; et al. Structural Insight into Substrate Preference for TET-Mediated Oxidation. *Nature* **2015**, *527*, 118–122. [[CrossRef](#)]
64. Zheng, G.; Dahl, J.A.; Niu, Y.; Fedorcsak, P.; Huang, C.-M.; Li, C.J.; Vågbo, C.B.; Shi, Y.; Wang, W.-L.; Song, S.-H.; et al. ALKBH5 Is a Mammalian RNA Demethylase That Impacts RNA Metabolism and Mouse Fertility. *Mol. Cell* **2013**, *49*, 18–29. [[CrossRef](#)] [[PubMed](#)]
65. Zhu, C.; Yi, C. Switching Demethylation Activities between AlkB Family RNA/DNA Demethylases through Exchange of Active-Site Residues. *Angew. Chem. Int. Ed.* **2014**, *53*, 3659–3662. [[CrossRef](#)]
66. Li, F.; Kennedy, S.; Hajian, T.; Gibson, E.; Seitova, A.; Xu, C.; Arrowsmith, C.H.; Vedadi, M. A Radioactivity-Based Assay for Screening Human M6A-RNA Methyltransferase, METTL3-METTL14 Complex, and Demethylase ALKBH5. *SLAS Discov.* **2016**, *21*, 290–297. [[CrossRef](#)]
67. Zou, S.; Toh, J.D.W.; Wong, K.H.Q.; Gao, Y.-G.; Hong, W.; Woon, E.C.Y. N6-Methyladenosine: A Conformational Marker That Regulates the Substrate Specificity of Human Demethylases FTO and ALKBH5. *Sci. Rep.* **2016**, *6*, 25677. [[CrossRef](#)]
68. Wang, L.; Song, C.; Wang, N.; Li, S.; Liu, Q.; Sun, Z.; Wang, K.; Yu, S.-C.; Yang, Q. NADP Modulates RNA M6A Methylation and Adipogenesis via Enhancing FTO Activity. *Nat. Chem. Biol.* **2020**, *16*, 1394–1402. [[CrossRef](#)]
69. Khatiwada, B.; Purslow, J.A.; Underbakke, E.S.; Venditti, V. N-Terminal Fusion of the N-Terminal Domain of Bacterial Enzyme I Facilitates Recombinant Expression and Purification of the Human RNA Demethylases FTO and Alkbh5. *Protein Expr. Purif.* **2020**, *167*, 105540. [[CrossRef](#)]
70. Mauer, J.; Luo, X.; Blanjoie, A.; Jiao, X.; Grozhik, A.V.; Patil, D.P.; Linder, B.; Pickering, B.F.; Vasseur, J.-J.; Chen, Q.; et al. Reversible Methylation of M6Am in the 5' Cap Controls mRNA Stability. *Nature* **2017**, *541*, 371–375. [[CrossRef](#)]
71. Ma, M.; Harding, H.P.; O'Rahilly, S.; Ron, D.; Yeo, G.S.H. Kinetic Analysis of FTO (Fat Mass and Obesity-Associated) Reveals That It Is Unlikely to Function as a Sensor for 2-Oxoglutarate. *Biochem. J.* **2012**, *444*, 183–187. [[CrossRef](#)] [[PubMed](#)]
72. Jia, G.; Yang, C.-G.; Yang, S.; Jian, X.; Yi, C.; Zhou, Z.; He, C. Oxidative Demethylation of 3-Methylthymine and 3-Methyluracil in Single-Stranded DNA and RNA by Mouse and Human FTO. *FEBS Lett.* **2008**, *582*, 3313–3319. [[CrossRef](#)] [[PubMed](#)]
73. Koivisto, P.; Duncan, T.; Lindahl, T.; Sedgwick, B. Minimal Methylated Substrate and Extended Substrate Range of *Escherichia coli* AlkB Protein, a 1-Methyladenine-DNA Dioxygenase. *J. Biol. Chem.* **2003**, *278*, 44348–44354. [[CrossRef](#)] [[PubMed](#)]
74. Yu, B.; Edstrom, W.C.; Benach, J.; Hamuro, Y.; Weber, P.C.; Gibney, B.R.; Hunt, J.F. Crystal Structures of Catalytic Complexes of the Oxidative DNA/RNA Repair Enzyme AlkB. *Nature* **2006**, *439*, 879–884. [[CrossRef](#)] [[PubMed](#)]
75. Roy, T.W.; Bhagwat, A.S. Kinetic Studies of *Escherichia coli* AlkB Using a New Fluorescence-Based Assay for DNA Demethylation. *Nucleic Acids Res.* **2007**, *35*, e147. [[CrossRef](#)]
76. Yu, B.; Hunt, J.F. Enzymological and Structural Studies of the Mechanism of Promiscuous Substrate Recognition by the Oxidative DNA Repair Enzyme AlkB. *Proc. Natl. Acad. Sci. USA* **2009**, *106*, 14315–14320. [[CrossRef](#)]
77. Ergel, B.; Gill, M.L.; Brown, L.; Yu, B.; Palmer, A.G.; Hunt, J.F. Protein Dynamics Control the Progression and Efficiency of the Catalytic Reaction Cycle of the *Escherichia coli* DNA-Repair Enzyme AlkB. *J. Biol. Chem.* **2014**, *289*, 29584–29601. [[CrossRef](#)]
78. Baldwin, M.R.; Admiraal, S.J.; O'Brien, P.J. Transient Kinetic Analysis of Oxidative Dealkylation by the Direct Reversal DNA Repair Enzyme AlkB. *J. Biol. Chem.* **2020**, *295*, 7317–7326. [[CrossRef](#)]
79. Wang, Y.; Katanski, C.D.; Watkins, C.; Pan, J.N.; Dai, Q.; Jiang, Z.; Pan, T. A High-Throughput Screening Method for Evolving a Demethylase Enzyme with Improved and New Functionalities. *Nucleic Acids Res.* **2021**, *49*, e30. [[CrossRef](#)]
80. Karkhanina, A.A.; Mecinović, J.; Musheev, M.U.; Krylova, S.M.; Petrov, A.P.; Hewitson, K.S.; Flashman, E.; Schofield, C.J.; Krylov, S.N. Direct Analysis of Enzyme-Catalyzed DNA Demethylation. *Anal. Chem.* **2009**, *81*, 5871–5875. [[CrossRef](#)] [[PubMed](#)]
81. Nigam, R.; Anindya, R. *Escherichia coli* Single-Stranded DNA Binding Protein SSB Promotes AlkB-Mediated DNA Dealkylation Repair. *Biochem. Biophys. Res. Commun.* **2018**, *496*, 274–279. [[CrossRef](#)]
82. Shivange, G.; Kodipelli, N.; Anindya, R. 2-Hydrazinobenzothiazole-Based Etheno-Adduct Repair Protocol (HERP): A Method for Quantitative Determination of Direct Repair of Etheno-Bases. *DNA Repair* **2015**, *28*, 8–13. [[CrossRef](#)] [[PubMed](#)]
83. Wei, Y.-F.; Carter, K.C.; Wang, R.-P.; Shell, B.K. Molecular Cloning and Functional Analysis of a Human cDNA Encoding an *Escherichia coli* AlkB Homolog, a Protein Involved in DNA Alkylation Damage Repair. *Nucleic Acids Res.* **1996**, *24*, 931–937. [[CrossRef](#)] [[PubMed](#)]
84. Yi, C.; He, C. DNA Repair by Reversal of DNA Damage. *Cold Spring Harb. Perspect. Biol.* **2013**, *5*, a012575. [[CrossRef](#)]
85. Ougland, R.; Lando, D.; Jonson, I.; Dahl, J.A.; Moen, M.N.; Nordstrand, L.M.; Rognes, T.; Lee, J.T.; Klungland, A.; Kouzarides, T.; et al. ALKBH1 Is a Histone H2A Dioxygenase Involved in Neural Differentiation. *Stem Cells* **2012**, *30*, 2672–2682. [[CrossRef](#)]
86. Ma, C.-J.; Ding, J.-H.; Ye, T.-T.; Yuan, B.-F.; Feng, Y.-Q. AlkB Homologue 1 Demethylates N³-Methylcytidine in mRNA of Mammals. *ACS Chem. Biol.* **2019**, *14*, 1418–1425. [[CrossRef](#)]

87. Westbye, M.P.; Feyzi, E.; Aas, P.A.; Vågbø, C.B.; Talstad, V.A.; Kavli, B.; Hagen, L.; Sundheim, O.; Akbari, M.; Liabakk, N.-B.; et al. Human AlkB Homolog 1 Is a Mitochondrial Protein That Demethylates 3-Methylcytosine in DNA and RNA. *J. Biol. Chem.* **2008**, *283*, 25046–25056. [\[CrossRef\]](#)
88. Haag, S.; Sloan, K.E.; Ranjan, N.; Warda, A.S.; Kretschmer, J.; Blessing, C.; Hübner, B.; Seikowski, J.; Dennerlein, S.; Rehling, P.; et al. NSUN3 and ABH1 Modify the Wobble Position of Mt-TRN^{Met} to Expand Codon Recognition in Mitochondrial Translation. *EMBO J.* **2016**, *35*, 2104–2119. [\[CrossRef\]](#)
89. Kawarada, L.; Suzuki, T.; Ohira, T.; Hirata, S.; Kenjyo, M.; Suzuki, T. ALKBH1 Is an RNA Dioxygenase Responsible for Cytoplasmic and Mitochondrial tRNA Modifications. *Nucleic Acids Res.* **2017**, *45*, 7401–7415. [\[CrossRef\]](#) [\[PubMed\]](#)
90. Wu, T.P.; Wang, T.; Seetin, M.G.; Lai, Y.; Zhu, S.; Lin, K.; Liu, Y.; Byrum, S.D.; Mackintosh, S.G.; Zhong, M.; et al. DNA Methylation on N6-Adenine in Mammalian Embryonic Stem Cells. *Nature* **2016**, *532*, 329–333. [\[CrossRef\]](#)
91. Liu, F.; Clark, W.; Luo, G.; Wang, X.; Fu, Y.; Wei, J.; Wang, X.; Hao, Z.; Dai, Q.; Zheng, G.; et al. ALKBH1-Mediated tRNA Demethylation Regulates Translation. *Cell* **2016**, *167*, 816–828.e16. [\[CrossRef\]](#)
92. Yang, C.-G.; Yi, C.; Duguid, E.M.; Sullivan, C.T.; Jian, X.; Rice, P.A.; He, C. Crystal Structures of DNA/RNA Repair Enzymes AlkB and ABH2 Bound to DsDNA. *Nature* **2008**, *452*, 961–965. [\[CrossRef\]](#) [\[PubMed\]](#)
93. Monsen, V.T.; Sundheim, O.; Aas, P.A.; Westbye, M.P.; Sousa, M.M.L.; Slupphaug, G.; Krokan, H.E. Divergent β -Hairpins Determine Double-Strand versus Single-Strand Substrate Recognition of Human AlkB-Homologues 2 and 3. *Nucleic Acids Res.* **2010**, *38*, 6447–6455. [\[CrossRef\]](#) [\[PubMed\]](#)
94. Chen, B.; Liu, H.; Sun, X.; Yang, C.-G. Mechanistic Insight into the Recognition of Single-Stranded and Double-Stranded DNA Substrates by ABH2 and ABH3. *Mol. BioSyst.* **2010**, *6*, 2143. [\[CrossRef\]](#) [\[PubMed\]](#)
95. Chen, F.; Tang, Q.; Bian, K.; Humulock, Z.T.; Yang, X.; Jost, M.; Drennan, C.L.; Essigmann, J.M.; Li, D. Adaptive Response Enzyme AlkB Preferentially Repairs 1-Methylguanine and 3-Methylthymine Adducts in Double-Stranded DNA. *Chem. Res. Toxicol.* **2016**, *29*, 687–693. [\[CrossRef\]](#)
96. Bian, K.; Lenz, S.A.P.; Tang, Q.; Chen, F.; Qi, R.; Jost, M.; Drennan, C.L.; Essigmann, J.M.; Wetmore, S.D.; Li, D. DNA Repair Enzymes ALKBH2, ALKBH3, and AlkB Oxidize 5-Methylcytosine to 5-Hydroxymethylcytosine, 5-Formylcytosine and 5-Carboxylcytosine in Vitro. *Nucleic Acids Res.* **2019**, *47*, 5522–5529. [\[CrossRef\]](#)
97. You, C.; Wang, P.; Nay, S.L.; Wang, J.; Dai, X.; O'Connor, T.R.; Wang, Y. Roles of Aag, Alkbh2, and Alkbh3 in the Repair of Carboxymethylated and Ethylated Thymidine Lesions. *ACS Chem. Biol.* **2016**, *11*, 1332–1338. [\[CrossRef\]](#)
98. Sundheim, O.; Vågbø, C.B.; Bjørås, M.; Sousa, M.M.L.; Talstad, V.; Aas, P.A.; Drabløs, F.; Krokan, H.E.; Tainer, J.A.; Slupphaug, G. Human ABH3 Structure and Key Residues for Oxidative Demethylation to Reverse DNA/RNA Damage. *EMBO J.* **2006**, *25*, 3389–3397. [\[CrossRef\]](#)
99. Chen, Z.; Qi, M.; Shen, B.; Luo, G.; Wu, Y.; Li, J.; Lu, Z.; Zheng, Z.; Dai, Q.; Wang, H. Transfer RNA Demethylase ALKBH3 Promotes Cancer Progression via Induction of tRNA-Derived Small RNAs. *Nucleic Acids Res.* **2019**, *47*, 2533–2545. [\[CrossRef\]](#)
100. Dango, S.; Mosammaparast, N.; Sowa, M.E.; Xiong, L.-J.; Wu, F.; Park, K.; Rubin, M.; Gygi, S.; Harper, J.W.; Shi, Y. DNA Unwinding by ASCC3 Helicase Is Coupled to ALKBH3-Dependent DNA Alkylation Repair and Cancer Cell Proliferation. *Mol. Cell* **2011**, *44*, 373–384. [\[CrossRef\]](#)
101. Brickner, J.R.; Soll, J.M.; Lombardi, P.M.; Vågbø, C.B.; Mudge, M.C.; Oyeniran, C.; Rabe, R.; Jackson, J.; Sullender, M.E.; Blazosky, E.; et al. A Ubiquitin-Dependent Signalling Axis Specific for ALKBH-Mediated DNA Dealkylation Repair. *Nature* **2017**, *551*, 389–393. [\[CrossRef\]](#) [\[PubMed\]](#)
102. Meyer, K.D.; Saletore, Y.; Zumbo, P.; Elemento, O.; Mason, C.E.; Jaffrey, S.R. Comprehensive Analysis of mRNA Methylation Reveals Enrichment in 3' UTRs and near Stop Codons. *Cell* **2012**, *149*, 1635–1646. [\[CrossRef\]](#) [\[PubMed\]](#)
103. Dominissini, D.; Moshitch-Moshkovitz, S.; Schwartz, S.; Salmon-Divon, M.; Ungar, L.; Osenberg, S.; Cesarkas, K.; Jacob-Hirsch, J.; Amariglio, N.; Kupiec, M.; et al. Topology of the Human and Mouse M6A RNA Methylomes Revealed by M6A-Seq. *Nature* **2012**, *485*, 201–206. [\[CrossRef\]](#) [\[PubMed\]](#)
104. Ensfielder, T.T.; Kurz, M.Q.; Iwan, K.; Geiger, S.; Matheisl, S.; Müller, M.; Beckmann, R.; Carell, T. ALKBH5-Induced Demethylation of Mono- and Dimethylated Adenosine. *Chem. Commun.* **2018**, *54*, 8591–8593. [\[CrossRef\]](#)
105. Takahashi, H.; Hase, H.; Yoshida, T.; Tashiro, J.; Hirade, Y.; Kitae, K.; Tsujikawa, K. Discovery of Two Novel ALKBH5 Selective Inhibitors That Exhibit Uncompetitive or Competitive Type and Suppress the Growth Activity of Glioblastoma Multiforme. *Chem. Biol. Drug Des.* **2022**, *100*, 1–12. [\[CrossRef\]](#)
106. Frayling, T.M.; Timpson, N.J.; Weedon, M.N.; Zeggini, E.; Freathy, R.M.; Lindgren, C.M.; Perry, J.R.B.; Elliott, K.S.; Lango, H.; Rayner, N.W.; et al. A Common Variant in the FTO Gene Is Associated with Body Mass Index and Predisposes to Childhood and Adult Obesity. *Science* **2007**, *316*, 889–894. [\[CrossRef\]](#)
107. Gerken, T.; Girard, C.A.; Tung, Y.-C.L.; Webby, C.J.; Saudek, V.; Hewitson, K.S.; Yeo, G.S.H.; McDonough, M.A.; Cunliffe, S.; McNeill, L.A.; et al. The Obesity-Associated FTO Gene Encodes a 2-Oxoglutarate-Dependent Nucleic Acid Demethylase. *Science* **2007**, *318*, 1469–1472. [\[CrossRef\]](#)
108. Wei, J.; Liu, F.; Lu, Z.; Fei, Q.; Ai, Y.; He, P.C.; Shi, H.; Cui, X.; Su, R.; Klungland, A.; et al. Differential M6A, M6Am, and M1A Demethylation Mediated by FTO in the Cell Nucleus and Cytoplasm. *Mol. Cell* **2018**, *71*, 973–985.e5. [\[CrossRef\]](#) [\[PubMed\]](#)
109. Fu, Y.; Jia, G.; Pang, X.; Wang, R.N.; Wang, X.; Li, C.J.; Smemo, S.; Dai, Q.; Bailey, K.A.; Nobrega, M.A.; et al. FTO-Mediated Formation of N6-Hydroxymethyladenosine and N6-Formyladenosine in Mammalian RNA. *Nat. Commun.* **2013**, *4*, 1798. [\[CrossRef\]](#)

110. Chen, W.; Zhang, L.; Zheng, G.; Fu, Y.; Ji, Q.; Liu, F.; Chen, H.; He, C. Crystal Structure of the RNA Demethylase ALKBH5 from Zebrafish. *FEBS Lett.* **2014**, *588*, 892–898. [\[CrossRef\]](#)
111. Waheed, S.O.; Ramanan, R.; Chaturvedi, S.S.; Ainsley, J.; Evison, M.; Ames, J.M.; Schofield, C.J.; Christov, C.Z.; Karabancheva-Christova, T.G. Conformational Flexibility Influences Structure–Function Relationships in Nucleic Acid N-Methyl Demethylases. *Org. Biomol. Chem.* **2019**, *17*, 2223–2231. [\[CrossRef\]](#) [\[PubMed\]](#)
112. Wang, B.; Cao, Z.; Sharon, D.A.; Shaik, S. Computations Reveal a Rich Mechanistic Variation of Demethylation of N-Methylated DNA/RNA Nucleotides by FTO. *ACS Catal.* **2015**, *5*, 7077–7090. [\[CrossRef\]](#)
113. Adams, J.M.; Cory, S. Modified Nucleosides and Bizarre 5'-Termini in Mouse Myeloma mRNA. *Nature* **1975**, *255*, 28–33. [\[CrossRef\]](#)
114. Wei, C.-M.; Gershowitz, A.; Moss, B. N⁶, O^{2'}-Dimethyladenosine a Novel Methylated Ribonucleoside next to the 5' Terminal of Animal Cell and Virus MRNAs. *Nature* **1975**, *257*, 251–253. [\[CrossRef\]](#) [\[PubMed\]](#)
115. Cliffe, L.J.; Siegel, T.N.; Marshall, M.; Cross, G.A.M.; Sabatini, R. Two Thymidine Hydroxylases Differentially Regulate the Formation of Glucosylated DNA at Regions Flanking Polymerase II Polycistronic Transcription Units throughout the Genome of *Trypanosoma Brucei*. *Nucleic Acids Res.* **2010**, *38*, 3923–3935. [\[CrossRef\]](#) [\[PubMed\]](#)
116. Vainio, S.; Genest, P.-A.; ter Riet, B.; van Luenen, H.; Borst, P. Evidence That J-Binding Protein 2 Is a Thymidine Hydroxylase Catalyzing the First Step in the Biosynthesis of DNA Base J. *Mol. Biochem. Parasitol.* **2009**, *164*, 157–161. [\[CrossRef\]](#)
117. van Leeuwen, F.; Taylor, M.C.; Mondragon, A.; Moreau, H.; Gibson, W.; Kieft, R.; Borst, P. β -D-Glucosyl-Hydroxymethyluracil Is a Conserved DNA Modification in Kinetoplastid Protozoans and Is Abundant in Their Telomeres. *Proc. Natl. Acad. Sci. USA* **1998**, *95*, 2366–2371. [\[CrossRef\]](#)
118. Toaldo, C.B.; Kieft, R.; Dirks-Mulder, A.; Sabatini, R.; van Luenen, H.G.A.M.; Borst, P. A Minor Fraction of Base J in Kinetoplastid Nuclear DNA Is Bound by the J-Binding Protein 1. *Mol. Biochem. Parasitol.* **2005**, *143*, 111–115. [\[CrossRef\]](#)
119. Torabifard, H.; Cisneros, G.A. Insight into Wild-Type and T1372E TET2-Mediated 5hmC Oxidation Using Ab Initio QM/MM Calculations. *Chem. Sci.* **2018**, *9*, 8433–8445. [\[CrossRef\]](#)
120. Waheed, S.O.; Chaturvedi, S.S.; Karabancheva-Christova, T.G.; Christov, C.Z. Catalytic Mechanism of Human Ten-Eleven Translocation-2 (TET2) Enzyme: Effects of Conformational Changes, Electric Field, and Mutations. *ACS Catal.* **2021**, *11*, 3877–3890. [\[CrossRef\]](#)
121. Waheed, S.O.; Varghese, A.; Chaturvedi, S.S.; Karabancheva-Christova, T.G.; Christov, C.Z. How Human TET2 Enzyme Catalyzes the Oxidation of Unnatural Cytosine Modifications in Double-Stranded DNA. *ACS Catal.* **2022**, *12*, 5327–5344. [\[CrossRef\]](#) [\[PubMed\]](#)
122. Liu, M.Y.; Torabifard, H.; Crawford, D.J.; DeNizio, J.E.; Cao, X.-J.; Garcia, B.A.; Cisneros, G.A.; Kohli, R.M. Mutations along a TET2 Active Site Scaffold Stall Oxidation at 5-Hydroxymethylcytosine. *Nat. Chem. Biol.* **2017**, *13*, 181–187. [\[CrossRef\]](#) [\[PubMed\]](#)
123. Kataoka, H.; Yamamoto, Y.; Sekiguchi, M. A New Gene (AlkB) of *Escherichia coli* That Controls Sensitivity to Methyl Methane Sulfonate. *J. Bacteriol.* **1983**, *153*, 1301–1307. [\[CrossRef\]](#)
124. Wang, J.; Qi, R.; Li, H.; Christov, C.; Lehnert, N.; Li, D. Genetic and Epigenetic Biomarkers Related to 2-Oxoglutarate/Fe(II)-Dependent Oxygenases and Implications for Disease and Toxicology. In *Biomarkers in Toxicology*; Patel, V.B., Preedy, V.R., Rajendram, R., Eds.; Biomarkers in Disease: Methods, Discoveries and Applications; Springer International Publishing: Cham, Switzerland, 2022; pp. 1–28. [\[CrossRef\]](#)
125. Fang, D.; Cisneros, G.A. Alternative Pathway for the Reaction Catalyzed by DNA Dealkylase AlkB from Ab Initio QM/MM Calculations. *J. Chem. Theory Comput.* **2014**, *10*, 5136–5148. [\[CrossRef\]](#) [\[PubMed\]](#)
126. Quesne, M.G.; Latifi, R.; Gonzalez-Ovalle, L.E.; Kumar, D.; de Visser, S.P. Quantum Mechanics/Molecular Mechanics Study on the Oxygen Binding and Substrate Hydroxylation Step in AlkB Repair Enzymes. *Chem.—A Eur. J.* **2014**, *20*, 435–446. [\[CrossRef\]](#)
127. Fang, D.; Lord, R.L.; Cisneros, G.A. Ab Initio QM/MM Calculations Show an Intersystem Crossing in the Hydrogen Abstraction Step in Dealkylation Catalyzed by AlkB. *J. Phys. Chem. B* **2013**, *117*, 6410–6420. [\[CrossRef\]](#) [\[PubMed\]](#)
128. Wang, B.; Usharani, D.; Li, C.; Shaik, S. Theory Uncovers an Unusual Mechanism of DNA Repair of a Lesioned Adenine by AlkB Enzymes. *J. Am. Chem. Soc.* **2014**, *136*, 13895–13901. [\[CrossRef\]](#)
129. Dai, Q.; Zheng, G.; Schwartz, M.H.; Clark, W.C.; Pan, T. Selective Enzymatic Demethylation of N²,N²-Dimethylguanosine in RNA and Its Application in High-Throughput tRNA Sequencing. *Angew. Chem. Int. Ed.* **2017**, *56*, 5017–5020. [\[CrossRef\]](#)
130. Li, M.-M.; Nilsen, A.; Shi, Y.; Fusser, M.; Ding, Y.-H.; Fu, Y.; Liu, B.; Niu, Y.; Wu, Y.-S.; Huang, C.-M.; et al. ALKBH4-Dependent Demethylation of Actin Regulates Actomyosin Dynamics. *Nat. Commun.* **2013**, *4*, 1832. [\[CrossRef\]](#)
131. Mielecki, D.; Zugaj, D.Ł.; Muszewska, A.; Piwowarski, J.; Chojnacka, A.; Mielecki, M.; Nieminuszczy, J.; Grynberg, M.; Grzesiuk, E. Novel AlkB Dioxygenases—Alternative Models for In Silico and In Vivo Studies. *PLoS ONE* **2012**, *7*, e30588. [\[CrossRef\]](#)
132. Tsujikawa, K.; Koike, K.; Kitae, K.; Shinkawa, A.; Arima, H.; Suzuki, T.; Tsuchiya, M.; Makino, Y.; Furukawa, T.; Konishi, N.; et al. Expression and Sub-Cellular Localization of Human ABH Family Molecules. *J. Cell. Mol. Med.* **2007**, *11*, 1105–1116. [\[CrossRef\]](#) [\[PubMed\]](#)
133. Zhang, L.-S.; Xiong, Q.-P.; Peña Perez, S.; Liu, C.; Wei, J.; Le, C.; Zhang, L.; Harada, B.T.; Dai, Q.; Feng, X.; et al. ALKBH7-Mediated Demethylation Regulates Mitochondrial Polycistronic RNA Processing. *Nat. Cell Biol.* **2021**, *23*, 684–691. [\[CrossRef\]](#) [\[PubMed\]](#)
134. Bobiak, M.L. Biochemical Characterization of Human AlkBH7. Doctoral Dissertation, Stony Brook University, Stony Brook, NY, USA, 2009.

-
135. Pastore, C.; Topalidou, I.; Forouhar, F.; Yan, A.C.; Levy, M.; Hunt, J.F. Crystal Structure and RNA Binding Properties of the RNA Recognition Motif (RRM) and AlkB Domains in Human AlkB Homolog 8 (ABH8), an Enzyme Catalyzing tRNA Hypermodification. *J. Biol. Chem.* **2012**, *287*, 2130–2143. [[CrossRef](#)] [[PubMed](#)]
136. Tang, Q.; Cai, A.; Bian, K.; Chen, F.; Delaney, J.C.; Adusumalli, S.; Bach, A.C.; Akhlaghi, F.; Cho, B.P.; Li, D. Characterization of Byproducts from Chemical Syntheses of Oligonucleotides Containing 1-Methyladenine and 3-Methylcytosine. *ACS Omega* **2017**, *2*, 8205–8212. [[CrossRef](#)] [[PubMed](#)]

Disclaimer/Publisher’s Note: The statements, opinions and data contained in all publications are solely those of the individual author(s) and contributor(s) and not of MDPI and/or the editor(s). MDPI and/or the editor(s) disclaim responsibility for any injury to people or property resulting from any ideas, methods, instructions or products referred to in the content.